ARCHIVIO ISTITUZIONALE
DELLA RICERCA

Alma Mater Studiorum Università di Bologna
Archivio istituzionale della ricerca

Hypogenic speleogenesis, late stage epigenic overprinting and condensation-corrosion in a complex cave system in relation to landscape evolution (Toirano, Liguria, Italy)

This is the final peer-reviewed author's accepted manuscript (postprint) of the following publication:

Published Version:
Columbu, A., Audra, P., Gázquez, F., D'Angeli, I.M., Bigot, J., Koltai, G., et al. (2021). Hypogenic speleogenesis, late stage epigenic overprinting and condensation-corrosion in a complex cave system in relation to landscape evolution (Toirano, Liguria, Italy). GEOMORPHOLOGY, 376, 1-10 [10.1016/j.geomorph.2020.107561].

Availability:
This version is available at: https://hdl.handle.net/11585/784100 since: 2021-01-08

Published:

DOI: http://doi.org/10.1016/j.geomorph.2020.107561

Terms of use:

Some rights reserved. The terms and conditions for the reuse of this version of the manuscript are specified in the publishing policy. For all terms of use and more information see the publisher's website.

This item was downloaded from IRIS Università di Bologna (https://cris.unibo.it/).
When citing, please refer to the published version.

(Article begins on next page)

14 November 2026

This is the final peer-reviewed accepted manuscript of:

Columbu, Andrea; Audra, Philippe; Gázquez, Fernando; D'angeli, Ilenia M.; Bigot, Jean-Yves; Koltai, Gabriella; Chiesa, Roberto; Yu, Tsai-Luen; Hu, Hsun-Ming; Shen, Chuan-Chou; Carbone, Cristina; Heresanu, Vasile; Nobécourt, Jean-Claude; De Waele, Jo: *Hypogenic speleogenesis, late stage epigenic overprinting and condensation-corrosion in a complex cave system in relation to landscape evolution (Toirano, Liguria, Italy)*

GEOMORPHOLOGY VOL 376 ISSN 0169-555X

DOI: 10.1016/j.geomorph.2020.107561

The final published version is available online at:
https://dx.doi.org/10.1016/j.geomorph.2020.107561

Terms of use:

Some rights reserved. The terms and conditions for the reuse of this version of the manuscript are specified in the publishing policy. For all terms of use and more information see the publisher's website.

This item was downloaded from IRIS Università di Bologna (https://cris.unibo.it/)

When citing, please refer to the published version.

Hypogenic speleogenesis, late stage epigenic overprinting and condensation-corrosion in a complex cave system in relation to landscape evolution (Toirano, Liguria, Italy)

Andrea COLUMBU ([a])*, Philippe AUDRA ([b]), Fernando GÁZQUEZ ([c]), Ilenia Maria D'ANGELI ([a]), Jean-Yves BIGOT ([d]), Gabriella KOLTAI ([j]), Roberto CHIESA ([e]), Tsai-Luen YU ([f]), Hsun-Ming HU ([f]), Chuan-Chou SHEN ([f]), Cristina CARBONE ([g]), Vasile HERESANU ([h]), Jean-Claude NOBÉCOURT ([d]), Jo DE WAELE ([a])

([a]) Dipartimento di Scienze Biologiche, Geologiche e Ambientali, Università di Bologna, Italy, jo.dewaele@unibo.it, andrea.columbu2@unibo.it, dangeli.ilenia89@gmail.com

([b]) University Côte d'Azur, Polytech'Lab - UPR 7498, Nice, France, Philippe.AUDRA@univ-cotedazur.fr

([c]) Department of Biology and Geology, University of Almeria, Spain, f.gazquez@ual.es

([d]) French Association of Karstology (AFK), France, jeanbigot536@gmail.com, jcnobecourt@free.fr

([e]) Gruppo Speleologico Cycnus, Toirano, Italy, bobchurch69@gmail.com

([f]) High-Precision Mass Spectrometry and Environmental Change Laboratory (HISPEC), Department of Geosciences, National Taiwan University, Taipei 10617, Taiwan ROC, d00224009@g.ntu.edu.tw, hsunming.hu@gmail.com, river@ntu.edu.tw

([g]) DISTAV, Università degli Studi di Genova, C.so Europa 26, 16132 Genova, Italy, cristina.carbone@unige.it

([h]) CINaM, CNRS – Aix Marseille University, Campus de Luminy, case 913, 13288 Marseille cedex 9, France, heresanu@cinam.univ-mrs.fr

([i]) Aix Marseille University, CNRS, IRD, Collège de France, INRAE, 13288 Marseille cedex 9, France, braucher@cerege.fr

([j]) Institute of Geology, University of Innsbruck, Innrain 52, 6020, Innsbruck, Austria,
gabriella.koltai@uibk.ac.at

(*) corresponding author

Keywords

Speleogenesis, hypogenic karst, dating, stable isotopes, landscape evolution

Abstract

The Toirano karst system is located in the Ligurian Alps, in the dolostones of Middle Triassic age, around 4.5 km inland from the coast (Borghetto Santo Spirito). It comprises different caves, among which the most important are, from the higher altitudes to the Varatella brook below, Colombo Cave (247 m asl), Upper Santa Lucia (215 m asl), Lower Santa Lucia (201 m asl), and the Bàsura Cave (186 m asl), the last two connected by an artificial tunnel and equipped for cave visits. Bàsura Cave is mainly known for the presence of cave bear bones and the footprints of Upper Paleolithic Man (12,000 years B.P.). Walking through the various environments and passages of the cave it is immediately clear that there is a very large variety of speleothems and morphologies. This geodiversity places Toirano caves among the most interesting and unique karst features of Italy. Up to only a couple of years ago, the genesis of the cave system was attributed to the action of underground rivers that would have created the complicated network of phreatic and vadose passages following the main tectonic features of the area. A more detailed investigation of the morphologies and sedimentary deposits, however, together with the presence of an active low thermal sulfidic spring (located on the important regional normal Mt. Carmo fault) only 500 m south of the caves and 100 m below the lowest passages in Bàsura Cave, favors the hypothesis of a hypogenic origin of the caves, by rising waters that followed the main vertical structural flow pathways that characterize the area. Many walls and roofs are sculpted with rising features (cupola

53 and megacusps); in other areas, despite the presence of copious speleothem deposits, vertical
54 feeders that brought the rising waters into the cave system have been localised. Most of the cave
55 voids would have formed close to the former water table (base) level, which was, given the close
56 distance from the sea, determined by the mean sea level at that time.
57 A series of geochronological analyses, including U/Th and cosmogenic burial dates have allowed
58 estimating the age of the highest lying cave (Colombo) at around 1.8 Ma (Gelasian). The age of this
59 cave level, now at 247 m asl, and the hypothesis of a sea level ca. 60 m lower than today, allow to
60 assess a mean uplift rate of the carbonate block north of the Mt. Carmo fault of 0.17 mm y^{-1}. Based
61 on these findings, Bàsura Cave might have formed ca. 1.4 Ma ago. Several U/Th dates on
62 speleothems have given ages beyond the limits of the method (>600 ka), confirming the system to
63 be rather old. The stable isotope analyses, on the other hand, indicate that the rising water was not
64 especially warm, with T values probably close to the current low-thermal spring in Toirano village,
65 i.e. around 22-23 °C. Besides uncovering the genesis of the Toirano karst system, this study
66 demonstrates that the combination of local geology, surface vs underground geomorphological
67 observations, climate change vs landscape evolution evaluation and geochemical data is of key
68 importance for interpreting subsurface land-shaping processes.
69

70 **1. Introduction**

71 The geological non-specialist community, as well as the public, is often unaware of the multiple
72 processes leading to cave formation. Indeed, speleogenesis is too often seen as the simple result of a
73 surface river infiltrating the bedrock through sinkholes, excavating the cave passages and then re-
74 emerging from karst springs. The action of bedrock dissolution in phreatic conditions along the
75 water table is also often taken for granted. Epigene caves are thus often arranged in levels, which
76 register the former base level (water table) stillstands (Palmer, 1987), and can thus help in
77 unravelling the landscape evolution of the areas in which they were carved (Calvet *et al.*, 2015;
78 Columbu *et al.*, 2015, 2017). However, the epigenic speleogenesis is only one of the several

79 modalities, actually the most common, by which "voids" can be formed underground. There is
80 increasing evidence showing that many caves form by rising fluids (thermal, rich in CO_2 or H_2S),
81 and classified as hypogene caves (Klimchouk, 2007). Hypogene caves can also form at former
82 water table levels, such as in the case of thermal caves (e.g. Budapest, Léel-Őssy, 2017), and
83 particularly in sulfuric acid (SAS) caves, where degassing of H_2S and oxidation is most efficient at
84 or immediately above the water surface (De Waele *et al.*, 2016). Hypogene-SAS caves are reliable
85 indicators of past water table levels and can help in determining base level changes, and especially
86 uplift rates (or related downcutting rates in adjacent valleys) (Piccini *et al.*, 2015; De Waele *et al.*,
87 2016; D'Angeli *et al.*, 2019).
88 The common epigenic origin is usually supported by the current presence of water streams in caves
89 and/or the "rounded" tunnels interpreted as phreatic conduits (Sauro et al., 2020). However, the
90 modern streams and the actual shape of natural underground tunnels can be the result of recent
91 geological events; the effective processes leading to cave formation must be traced further in the
92 past, i.e. when the initial fluids started enlarging the most permeable pathways, leading to the
93 selection of the most effective drainage routes (Ford and Williams, 2007; Palmer, 2007).
94 Furthermore, the geomorphological evidences of ancient speleogenesis can be partially lost because
95 of weathering, speleothem deposition, sedimentation, collapses, human activity, etc (Sauro et al.,
96 2019). There are processes such as condensation-corrosion, boosted by the presence of guano
97 and/or warm and moist air circulation in caves, which are greatly underestimated in the shaping of
98 caves (Audra *et al.*, 2016; Cailhol *et al.*, 2019; Dandurand *et al.*, 2019). These processes, instead,
99 can be extremely important in the late speleogenetic stages, especially when cave passages become
100 largely opened to the surface, concurrently erasing evidences coming from the deeper past.
101 Accordingly, the study of cave formation needs an accurate interpretation of underground
102 morphologies (tunnel shape, size, geometries; wall, ceiling and floor features; chemical precipitates
103 and sediments; etc.), which should also be supported by geochemical and stratigraphic analyses of
104 cave deposits (speleothems vs. sediments), considerations about the bedrock features (faults,

lineaments, bedding, etc.) and the geological status of the area (active tectonics, uplifting vs. subsidence, etc.), and evaluations about surface dynamics related to climate and landscape evolution (De Waele *et al.*, 2009; Audra and Palmer, 2015; Columbu *et al.*, 2015, 2017). Speleogenetic processes must be pinpointed in time, thus dating is a key for anchoring underground processes to a coherent geochronology (Sasowsky, 1998).

The Toirano karst system in Liguria, Northern Italy, displays multiple cave levels and an impressive variety of underground morphologies, as much as probably making it the Italian show cave with the highest geodiversity. It is located 4.5 km from the coastline at moderate altitude (150-350 m asl), in the dynamic geological context of the Western Alps. Ancient hominid groups frequented these caves. These features challenge a straightforward interpretation of its formation, although past local investigators have considered underground rivers as the main player. The presence of a nearby thermo-mineral spring suggests a possible influence of a deep flow component, and substantial differences in morphologies are indicative of processes associated to confined areas vs. passages strongly influenced by a connection to the surface, such as bat-related biocorrosion and condensation-corrosion.

The in-detail investigation of cave morphologies and stratigraphy, U-Th dating and stable isotope analyses of speleothems and cosmogenic burial dating of sediments, provide evidence leading to a different scenario of cave genesis, in a changing climate, environment and landscape.

We take the Toirano karst system as an example of an enigmatic case study to suggest a guideline in the investigation of cave evolution, based on a correct interpretation of underground morphologies, sustained by geochemical analyses, anchored in time by dating and coherently integrated with surface events. Our results allow reconstructing the evolution phases of the cave system during the Quaternary, witnessing profound changes in the surrounding landscape.

2. Study area

The Toirano karst system of develops, along the lower slopes of Mt. Carmo di Loano (1389 m asl), half a kilometre north of the small village of the same name (Savona Province, Liguria, north-western Italy) (Figure 1). The main entrance of one of the caves (Upper Santa Lucia) is well visible from a long distance (Gruppo Speleologico Cycnus & Delegazione Speleologica Ligure, 2001). The caves develop in the slopes on the hydrographic left of the Varatella torrent, at the outlet of its gorges, upstream of the coastal plain, the shoreline being located only 4.5 km downstream from the caves. This area belongs to the Briançonnais domain of the Ligurian Alps, being part of a complex dome structure dipping here 20-30° toward the NE (Boni *et al.*, 1971; Cavallo, 2001). The *San Pietro dei Monti* (Middle Triassic) constitutes the main local unit. Although mainly composed by dolostones, it presents a more calcareous lower formation (*Costa Losera Fm.*), in which most caves are carved. The direction of the cave passages is greatly controlled by the main fracture sets in the region with typical NE-SW directions (60% of all fractures), which are associated to the important uplift phases of Pliocene age, and minor components in the N-S (15%) and W-E directions (25%) (Sarigu, 2001). Toward the south, the carbonate rocks are interrupted by an important regional NE-SW fault with a vertical offset of at least 200 m, that places the Middle Triassic dolomites in contact with the quartzites of the *Ponte di Nava* Formation, Lower Triassic in age (Figure 2) (Menardi Noguera, 1984; Cavallo, 2001). It is along this major tectonic contact that the thermal spring of Toirano is located, on the hydrographic right side of the Varatella brook and at an altitude of 70 m asl. This spring has a rather high mean discharge of 100 $L.s^{-1}$ and delivers waters of 22-23 °C, with a slightly basic pH (7.2-7.4) and moderate mineralization (ca. 600 µS/cm at 20 °C, hardness of 23 °F); it consists in a bicarbonate-calcium type water with not negligible concentration in sulphates (25-37 mg L^{-1} SO_4^{2-}) (Calandri, 2001). These hydrogeochemical characteristics remain very stable year-round, including after important rain and flood events, which would exclude significant mixing with shallow meteoric water and surface runoff from the Varatella torrent. The isotopic signature of the thermal spring ($\delta^{18}O$ = -6,9 ‰ vs. -5,8 ‰ at the coast), points toward a mean

155 altitude of its catchment at around 400 m asl, corresponding to a surface of about 4 km^2 along the
156 slopes of Monte Carmo (Cavallo, 1990).
157 The Varatella torrent generated strath-like terraces that can be traced up to an altitude of ca. 100 m
158 asl (Fanucci et al., 1987). In the neighboring Ria of Albenga (5 km south of the study area) there are
159 remnants of two levels of Lower Pliocene shorelines located at 280-310 and 380-420 m asl,
160 showing a Plio-Quaternary uplift of the mountain front of at least 350-400 m (Marini, 2004).
161 Offshore, these Pliocene marine deposits, several hundreds of metres thick, are burying the deeply-
162 incised Messinian canyon of the Centa River (Clauzon *et al.*, 1996; Soulet *et al.*, 2016). In the
163 Varatella valley itself, Pliocene remnants are very scarce, limited to a conglomerate outcrop in a
164 small plateau (45 m asl) at the outlet of the highway tunnel (Boni *et al.*, 1971). Its visible part
165 displays as an inclined bank of cemented angular limestone blocks originating from the local hill,
166 resting on a sand bank. This conglomerate corresponds to lateral foresets of the Pliocene Gilbert
167 Delta filling the Messinian canyon of the Varatella river. The canyon can be traced offshore from
168 Borghetto San Spirito, where it flowed together with the Centa Messinian canyon originating from
169 the larger valley of Albenga (Soulet *et al.*, 2016). Apart from these conglomerates, there is no
170 indication of the inland extension of the Messinian Varatella canyon, which might have been
171 uplifted and probably eroded. Currently, in Toirano, the Varatella torrent flows directly on the
172 quartzite bedrock.
173 Climate in Toirano is mild Mediterranean and maritime, warm and temperate, with an average
174 annual temperature of 14.3 °C (mean minimum of 6.6 °C in January, mean maximum of 22.6 °C in
175 July); annual rainfall is 830 mm with no pronounced wet season, while June and August are
176 essentially dry.
177 The caves of Toirano are known since a very long time, and visitors have left their autographs on
178 the walls of Upper Santa Lucia Cave (*Grotta di Santa Lucia Superiore* or Sanctuary Cave) (215 m
179 asl, 378 m long) at least since the XV^{th} century. This explains the presence of the church
180 (Sanctuary) at the entrance of the cave, built between centuries XV and XVI. The other caves with a

181 relevant underground development in the area are Lower Santa Lucia Cave (*Grotta di Santa Lucia*
182 *Inferiore*, 201 m asl, 778 m long), the Bàsura Cave (*Grotta della Bàsura*, 186 m asl, 890 m long),
183 Colombo Cave (*Grotta di Colombo*, 247 m asl, 310 m long) (Chiesa, 2007) and the small Ulivo
184 Cave (*Grotta dell'Ulivo*, 337 m asl, 27 m long) (Gruppo Speleologico Cycnus e Delegazione
185 Speleologica Ligure, 2001) (Figure 1).
186 Archaeological digging carried out from the end of the XIXth century both in Bàsura and Colombo
187 caves, and in some nearby smaller caves, has shown these caves were fundamental sheltering places
188 for the first inhabitants in this coastal area (Morelli, 1890; Cauche, 2007). Many of the investigated
189 caves appear to have been used by ancient human groups at least starting from the Lower
190 Paleolithic (around 150×10^3 years before present, hereafter ka) (Arobba *et al.*, 2008), and some
191 bones of *Homo neanderthalensis* have been discovered in the Upper Santa Lucia Cave. It is general
192 belief among archaeologists that some of the older artefacts (Tayazian age) might have even been
193 constructed by the predecessor of the actual *Homo sapiens*, the *Homo heidelbergensis* (Negrino and
194 Tozzi, 2008).

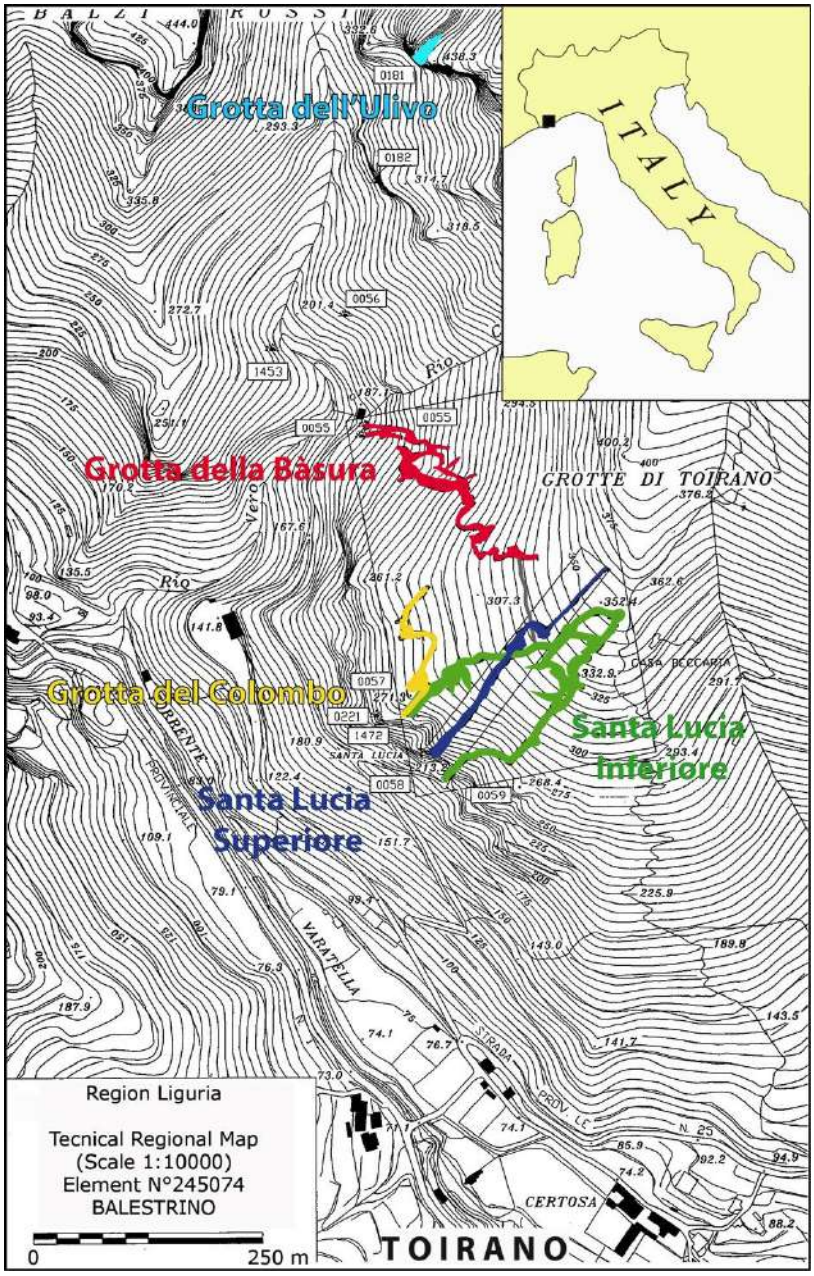

Figure 1. Location of the most important caves described in the text. The thermal spring is located some hundred metres south of the Certosa (just outside of this map). Numbers in white boxes refer to the cave register numbers of the Ligurian Speleological Federation.

The Bàsura Cave became famous in 1950 after some local people opened a narrow passage some tens of metres from the entrance with explosives, exploring a series of long corridors and rooms, which led to the discovery of human traces, including bare footprints, and a great number of bones of cave bears (*Ursus spelaeus*). The human footprints were initially ascribed to Neanderthal, but

radiometric dating and recent research with modern laser scanning techniques (Citton *et al.*, 2017) have allowed to ascertain that the traces belong to three individuals of Modern Humans that explored the cave more or less 12,000 years ago, for reasons still not entirely understood (Molleson *et al.*, 1972; De Lumley *et al.*, 1984).

Bàsura Cave was opened to the public in 1953, and in 1967 a 110-m-long artificial tunnel connected Bàsura with Lower Santa Lucia Cave (Gruppo Speleologico Cycnus e Delegazione Speleologica Ligure, 2001). These rather high-impact construction works, despite damaging part of the underground landscape, have allowed a more efficient management of the tourist visits, with shorter permanence of groups. Furthermore, the artificial digging for the tunnel has allowed discovering some new natural cave passages that would otherwise have remained unknown, since they do not have natural access. These impressive construction works have emptied the lake that was present in the *Antro di Cibele* in the lowest part of the known cave passages. The drying out of this lake has generated an important exchange of atmospheric masses between different cave branches, starting the circulation of large quantities of air in the cave environment, a process that was previously lacking.

Sarigu (2001) and Calandri (2001) have described the caves of the area from a geological, structural and geomorphological point of view, and gave the first detailed speleogenetic hypothesis. Most authors attribute cave formation to the Pliocene, related to the intense uplift of the region and the opening of the ENE-WSW fractures (Sarigu, 2001), although some authors even mention a start of cave-forming processes during the Lower Miocene (Fanucci, 1985). The extraordinary beauty and variety of speleothems, and the great morphological diversity between the different underground environments, suggest the caves have undergone a rather complex series of events and processes, justifying the following detailed studies.

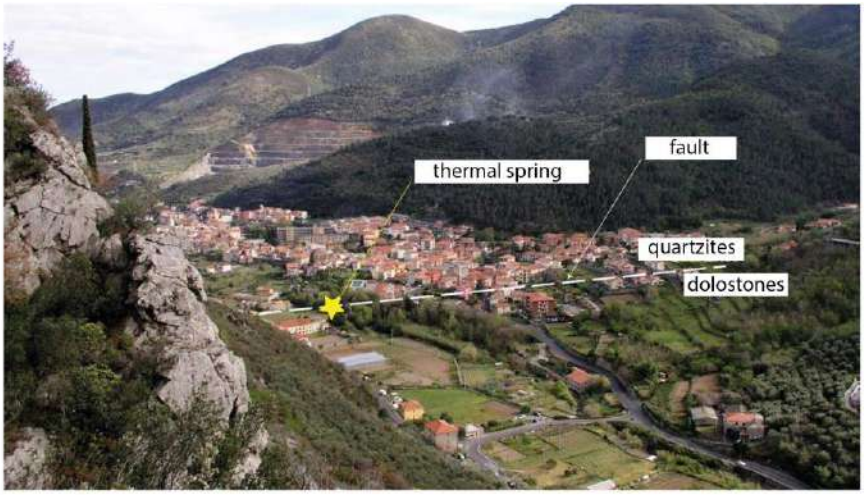

Figure 2 – View on Toirano village and on the Varatella torrent from the entrance of Colombo Cave. The Mediterranean shoreline is located 4.5 km southward, behind the last hills (Photo J.-Y. Bigot).

3. Methods

Toirano and its caves have been visited several times between 2015 and 2019 to carry out geomorphological observations in all passages (tourist trails, but also speleological branches where vertical rope techniques were needed). During these visits, sediments, speleothems and secondary minerals have been sampled in most caves (for locations of samples see Figure 3). Sediments and morphological features where considered with a stratigraphic approach, in order to attribute a relative chronology. Meantime, photographic documentation was taken. Following our conservational purposes (Columbu et al., 2020), almost all samples were taken from fragments found broken on the ground, result of the many constructional works carried out in the cave since 1953 and especially in the late 60s.

Minerals have been analyzed with classical techniques (X - Ray Diffractometry, Scanning electron microprobe analyses) at Genova University and at CINaM (CNRS - Aix-Marseille University) (more details on mineralogical analytical methods can be found in Audra *et al.*, 2019).

Some samples of quartz- and feldspar-containing sands have been sampled for Al-Be cosmogenic burial dating at the CEREGE-CNRS (Aix Marseille University) (for detailed analytical methods see Bella *et al.*, 2019). The sampling sites are located 50 m from the entrance of Colombo Cave, shielded by a vertical rock thickness of at least 100 m, therefore no post-production was taken into account in the burial age calculations. We assume that the samples were exposed at the surface over long times accumulating nuclide concentrations, which started decreasing by radioactive decay once the sediments were buried in the caves.

Samples fragments of speleothems have been dated by the U-series method at the University of Taiwan (for detailed methods see Shen *et al.*, 2012 and Columbu *et al.*, 2019), whereas stable isotopes were measured at the University of Cambridge (UK) and Almeria (Spain) (for details on methods see Gázquez *et al.*, 2018). A double-polished thick section have been prepared from a calcite raft sample of Cibele (Toirano Cave, TO19) for fluid inclusion petrography.

4. Results: cave morphologies and deposits

The caves and their deposits will be described separately starting from the highest (Colombo Cave) to the lowest (Bàsura Cave). For cave locations see Figure 1, while geochemical/dating, mineralogical results and morphological observations are summarised in tables 1, 2, 3 and 4, together with figures 4-7

4.1. Colombo Cave

This cave opens at 247 m asl and has a wide entrance (Figure 3A). Already at the entrance, patches of coarse alluvial sediment can be seen stuck on the limestone walls (Figure 4A). The rounded pebbles of these deposits are up to 5 cm in diameter, and they are cemented in a reddish matrix containing mica and quartz. The wide entrance passage was used during prehistoric times, and a 4.5 m-deep archaeological excavation pit is present at a little more than 10 m from the entrance (Figure 4B) (Arobba *et al.*, 2008). The stratigraphy of this exposed sedimentary sequence shows angular

elements (cryoclastic material that has almost not been moved from where it was formed, very different from the alluvial deposits described above), and some darker horizons related to periods of human occupation, and/or to old guano deposits. U/Th and ESR dating at 76-70 ka assign the lower part of the excavation to Marine Isotope Stage (MIS) 5 (Pirouelle, 2006). 25 m from the entrance, the cave turns abruptly to the NW and enters in a large room of 10 m wide. In the bend of the passage, some smaller ascending galleries open to the east. Alluvial deposits with rounded pebbles of ca. 2 cm diameter of local black dolomite and allogenic fluvial material (quartzite, green schists) in a mica-quartz matrix are present here. These are covered with a brown crust (TO11, apatite) together with an old calcite flowstone that covers the crust too (TO10, >600 ka; Table 3). At the entrance to the room, to the right and close to the roof, a series of cupola-like morphologies and ascending channels are highlighted by the presence of orange-coloured sandy sediments filling them partially (Figure 4C). In one of these, a calcite flowstone crust has been sampled (TO5, >600 ka), also reporting sands on its top (TO6). The sands contain mica and quartz, and are the finer counterpart of the alluvial sediments described above. On the western wall in front of these pockets an old corroded flowstone has been sampled (TO7, 375.5 ±14.7 ka) (Figure 4D), whereas another old flowstone sample has been taken in a corrosion pocket in the central room (TO8, 179.7 ±4.1 ka) (Figure 4E). The room is dominated by a large rock pillar standing at its center, being larger at its top and narrowing toward the floor (Figure 4F). The roof of the room and entrance passage is sculpted by cupolas and the rocks have an overall smooth and wavy appearance. Remnants of old corroded flowstones can be seen here and there along the walls.

The floor of the central room is covered by dark bat guano deposits, most of which seems to be rather old. Yellowish crusts (Figure 4G) and flowery overgrowths have shown the presence of typical minerals of guano decay, including gypsum, ardealite, and newberyite (Audra *et al.*, 2019) (Table 1).

Table 1. Mineralogy of samples taken in the different caves (C = Colombo; LSL = Lower Santa Lucia; B = Bàsura). Hm = Hydromagnesite; Hu = Huntite; Ar = Aragonite; Ca = Calcite; Do = Dolomite; Gy = Gypsum; Br = Brushite; Ard = Ardealite; Nb = Newberyite; Le = Leucophosphite; Sp = Spheniscidite; Ap = Fluorapatite or Hydroxylapatite; Q = Quartz; He = Hematite; Go = Goethite; Ma = Ti-magnetite; Il = Illite; Mu = Muscovite; Fs = Feldspar; Cl = Clinochlore

ID	Cave	Sampling site	Observations	Minerals
C1	C	Main room	Hard yellow crystals on guano	Gy, Nb
C2	C	New branch after gate	Recent calcite rafts	Ca
C3	C	Main room	Yellow soft material on guano	Ard, Br
TO6	C	Ceiling pocket at entrance of chamber	Cemented sand, younger than TO5	Detrital (Q, Mu)
TO9a	C	Main Chamber, inner wall	Yellow gypsum flower	Gy, Le + detrital (Q, Mu/Il)
TO9b	C	Main Chamber, inner wall	Beige phosphate deposit, drier than where gypsum is found	Gy, Le, He + detrital (Q, Mu/Il, Fs)
TO11	C	Side passage before chamber	Dark phosphate crust	Ap, Ca + detrital (Q, Mu/Il, Fs)
T5	LSL	Crystal Branch	White deposit on floor	Hm, Do
T6	LSL	Crystal Branch	White deposit on crystals on the wall	Hu, Hm, Do
T7	LSL	Crystal Branch	Weathered wall with boxwork	Ca, Ma
T8	LSL	Crystal Branch	Brick red weathering material	Ca + detrital (Q, He, Il, Cl)
T9	LSL	Crystal Branch	Yellowish pasty material	Ca
T10	LSL	Crystal Branch	Residual fluvial green-grey clay in fracture	Detrital (Q, Mu)
T11	LSL	Crystal Branch	Fluvial sediment	Do + detrital (Q, Mu, Cl)
TO12	LSL	Above Pozzo del Ade	Weathered wall	Detrital (Mu/Il, Fs), Go
TO16b	LSL	Gallery below Pantheon	Sandy progradant deposit below calcite (TO16a)	Rounded detrital elements (Q, quartzite, He/Go, Fs)
TO22	LSL	Tanone	Several samples of pebbles below old stalagmite	Rounded detrital elements (Q, quartzite, He/Go, Fs) in Ca cement
T1	B	Fascio, lower parts	White dots on the wall	Hm, Hu, Ar
T3	B	Base Cibele	Old thin stratified calcite rafts	Ca
T4	B	Top of Cibele, first room	Thick calcite rafts	Ca
TO17	B	Slope down to Cibele	Sand below white calcite (TO18)	Rounded detrital elements (Q, quartzite, He/Go, Fs)
TO21	B	Fascio, small inlet in entrance series	Brown phosphate crust	Ap + detrital (Q, Mu/Il)

The room turns into a more-narrow passage towards the NE, where the cave continues for over 250 m in rather narrow but well decorated and faintly active (wet) passages. Just before entering this branch, to the left, there are more sand-filled pockets. These sands have a composition similar to the ones described earlier (Figure 4H), but grainsize decreases. The decrease of grainsize moving

306 toward the cave interior testifies that water, which deposited this material, came from the entrance.
307 Al-Be burial dating of these sands has given an age of ~1.8 Ma (Tab. 4). This represents the
308 approximate age of all these allogenic sediments, which were injected into the Colombo Cave when
309 the river was at the same (or slightly higher) altitude than the entrance.
310 Proceeding into the cave the environments become much smaller. This part was discovered after
311 opening a flowstone plug that only left a centimetre-space for air to pass through. Nowadays a gate
312 closes this branch for conservation purposes. Behind the gate, the passages are characterised by
313 shallow pools fed by active speleothems, and a rather important air circulation. In one of the dried-
314 out pools, some calcite rafts have been sampled (C2), which stable isotopes indicate temperature of
315 precipitation around 20 °C (Table 2). The passage ends on a sediment plug, thus the morphology of
316 the conduit and the type of flow at the origin of the initial passage is not visible.

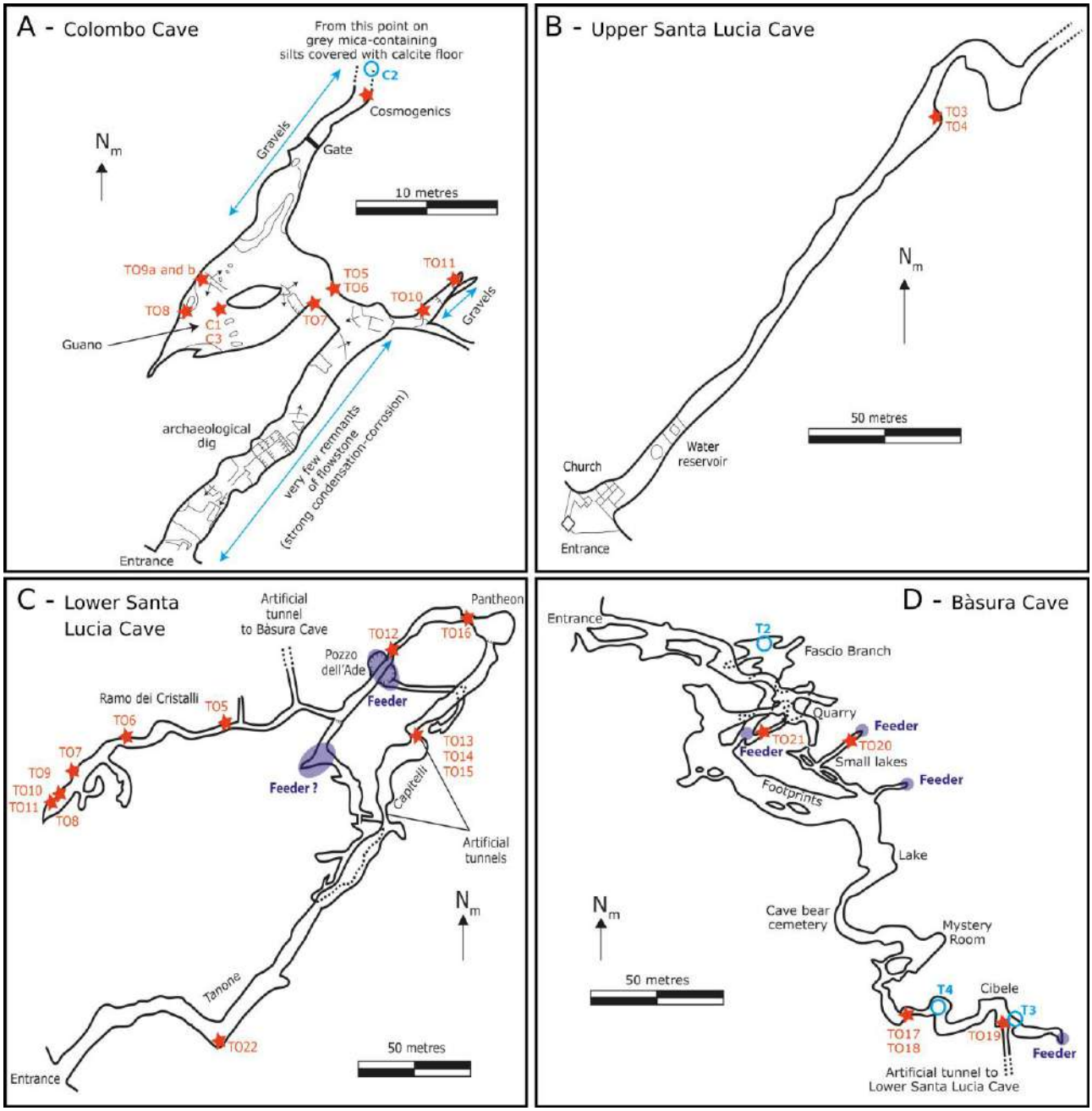

317

318 *Figure 3 – Simplified plan view of the entrance parts of Colombo Cave (A), Upper Santa Lucia*

319 *Cave (B), Lower Santa Lucia Cave (C) and Bàsura Cave (Dsampling locations and othe useful*

320 *information are reported (Survey courtesy of Gruppo Speleologico Cycnus e Delegazione*

321 *Speleologica Ligure, 2001).*

322

323 *Table 2. Stable isotopes and estimated paleo-temperatures (local $\delta^{18}O_w$ = -5.8 ‰, from Cavallo,*

324 *1990). (C = Colombo; B = Bàsura).*

ID	Cave	Place	$\delta^{18}O$	$\delta^{13}C$	T °C (with $\delta^{18}O_w$ = -5.8)	T °C (with $\delta^{18}O_w$ = -4)
C2	C	Old calcite raft	-5.90	-8.24	16	24
T2	B	Active calcite raft	-5.37	-10.02	14	22
T3	B	Calcite raft, lower part of Cibele	-4.98	-9.66	16	20
T4	B	Calcite raft, upper part of Cibele	-5.70	-10.65	13	23
TO18	B	Old flowstone (>600 ka), Upper Cibele	-5.12	-8.17	13	21
TO19	B	Old flowstone (562 ka), Lower Cibele	-5.24	-9.32	14	21
TO20	B	Recent mammalies (35 ka), Lakes	-4.40	-9.09	10	18

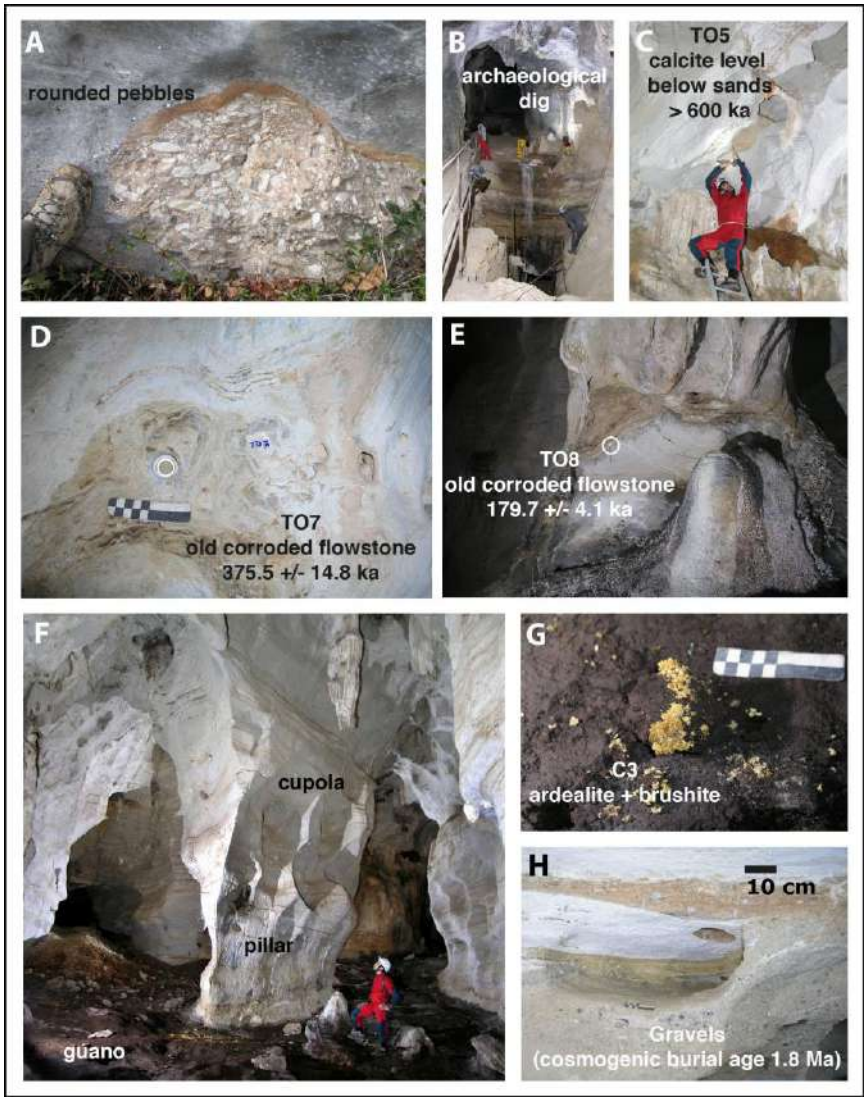

Figure 4 – Morphologies and deposits in Colombo Cave (Photos by Jean-Yves Bigot): A. Cemented pebble deposit in a reddish loamy matrix, found outside at the entrance of Colombo Cave; B. The

archaeological excavation pit a few metres from the entrance; C. Rising cupolas filled with a calcite coating (TO5) and a sandy deposit (TO6); D. Old corroded flowstone (TO7) at the entrance of the large room; E. Old flowstone (TO8) sampled on the western wall of the room; F. Overview of the central large room with the pillar, cupola on the ceiling, and abundant guano deposits; G. Yellowish secondary minerals on guano (ardealite and brushite); H. Gravels sampled for cosmogenic burial dating (1.8 Ma) (B/W scale in centre of photo).

Table 3. U/Th dating of samples taken in the different caves (C = Colombo; USL = Upper Santa Lucia; LSL = Lower Santa Lucia; B = Bàsura)

ID	Cave	Age (ka B.P.)	Sampling site	Observations
TO5	C	>600	Entrance Central Room	Calcite layer older than TO6
TO7	C	375.5 ±14.8	Entrance Central Room	Corroded flowstone
TO8	C	179.7 ±4.1	Central Room	Old corroded calcite in pocket
TO10	C	>600	Lateral branch of Central Room	Old white calcite floor
TO3	USL	407.6 ±22	After station 10	Old stalagmite
TO4	USL	343.0 ±10.4	After station 10	Border of less old rimstone dam
TO13	LSL	>600	Entrance *Capitelli*	Subaqueous calcite older than TO14
TO14	LSL	577.2 ±60.6	Entrance *Capitelli*	Pool calcite, younger than TO13
TO15	LSL	541.4 ±105.5	Entrance *Capitelli*	Upper part of *Capitello*
TO16	LSL	581.3 ±143.3	Passage below Pantheon	Calcite layer on sands
TO18	B	>600	Down to Cibele	White calcite covering sands of TO17
TO19	B	562.3 ± 77.1	Bottom Cibele before tunnel	Old subaqueous calcite in Cibele
TO20	B	35.1 ± 0.3	Small Lakes	Mammillary calcite

Table 4. Cosmogenic burial age of quartz gravels in Colombo Cave (C). (*) = upper limit in ^{10}Be. ASTER, 5MV AMS facility.

ID	Cave	Sampling site	^{10}Be (at/g)	^{26}Al (at/g)	Burial age (Ma)
TO	C	Inner wall of central room	8 453*	24 621 ± 15 053	1.798 ±1.1

342 **4.1.2. Upper Santa Lucia Cave**

343 The enormous entrance of the Upper Santa Lucia Cave (215 m asl) is visible from miles away, also
344 because in the XVth century church has been built in its entrance (Figures 3B and 5A). Pilgrims
345 visited the site for over six centuries (Figure 5B). The first 50 m of the large entrance are occupied
346 by the still active church, and behind the altar there is an artificial basin that collects dripping water.
347 Visits were initially possible using candles, then carbide lamps, the reason why the floor and walls
348 have become blackened by soot (Figure 5C-D). The cave continues behind the altar. The roof of the
349 inner cave passage is characterised by a never-ending network of interpenetrating cupola, while
350 most of the cave shows strong effects of corrosion as evidenced by smoothed walls and visible
351 deep-inner rings of flowstones (Figure 5D-E). The floor is covered with patches of old guano
352 (Figure 5D), and it is clear that large bat colonies inhabited the cave in the past. The passage ends in
353 an old flowstone, which has been damaged by explosives, probably in the hope of finding a
354 continuation of the cave. These "exploration" attempts however failed. Consequently, the
355 characteristics of the original passage feeding the cave cannot be investigated. The remnants of an
356 old corroded flowstone (TO3) and a slightly younger rimstone (TO4) have been sampled, giving
357 ages of 407.6 ±22 and 343.0 ±10.4 ka, respectively (Figure 5F) (Table 3).
358

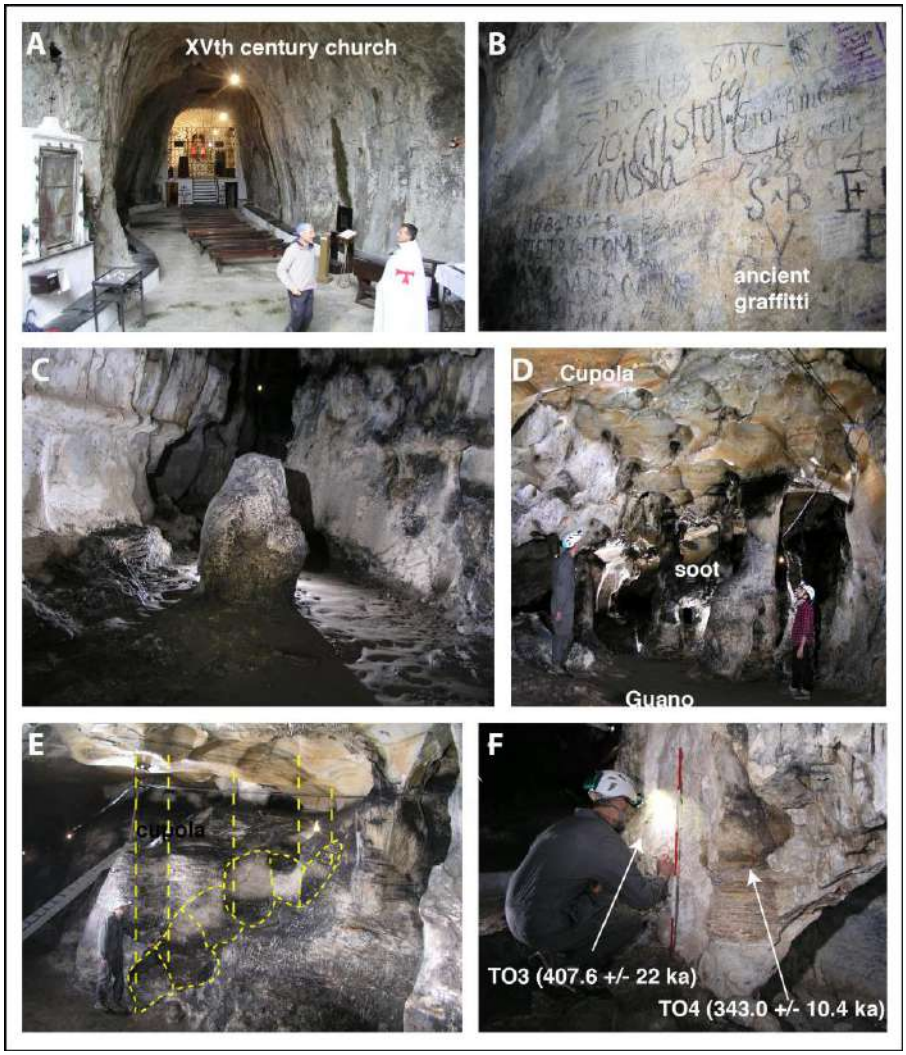

Figure 5 – Morphologies in Upper Santa Lucia Cave (Photos by Jean-Yves Bigot): A. The XVth century church in the wide entrance part of the cave; left to the altar, a door closes the inner part; B. Graffiti on the walls in the inner cave (note writings of year 1687 to the left); C. Strongly corroded stalagmite (1.5 m tall) with growth rings highlighted by soot veneer. Lateral calcite shelves, similar to TO4, recording an ancient pool level, are visible on the walls; D. The final part of the cave with corroded speleothems, coalescing cupolas, remnants of black soot on the walls, and a floor covered with old bat guano; E. Biocorrosion cupolas (derived from bat and guano) and dripping-pots, which are developing at the vertical of ceiling pendants that concentrate condensation runoff; F. The sampled old flowstone (TO3) and the younger rimstone deposits (TO4).

4.1.3. Lower Santa Lucia Cave

Lower Santa Lucia Cave is located at 201 m asl, 14 m below and slightly south of the Upper Santa Lucia Cave (Figure 3C). It is a perfectly horizontal over 5 m wide and 10 m high passage, with smooth corroded walls of a powdery dry aspect, and with almost no speleothems, except for a few old corroded and massive flowstones. It looks more like a mining tunnel than a natural cave (Figure 6A). In the past, it harboured large bat colonies, as indicated by remnants of phosphate crusts in cupolas. A pebble deposit has been sampled (TO22) below one of the old flowstones. Some quartzite gravels clearly show an external origin from fluvial material (Figure 6B).

Approximately 200 m from the entrance, a narrow passage equipped with a door isolates the inner part of the cave from the external air. Behind this door, the cave appears as a completely different environment with respect to the outer part. A little further into the cave, the floor is scattered with mushroom-like speleothems, with a series of shelfstone levels growing at different heights above the cave floor, culminating in a more extensively developed shelfstone level at 1.7 m height, forming the hats of the mushrooms (Capitelli) (Figure 6C). These testify to the presence in the past of large pools where outgassing caused the slow deposition of mammillary calcite and shelfstones (De Waele et al., 2018). The stipe of the “mushrooms”, because of their typical steep conical shape, is probably formed by up-to-2-metre high raft cones, although none is broken so they might also be common stalagmites. Three calcite samples have been taken here for U/Th dating: an old white subaqueous mammillary calcite deposit stratigraphically being first to grow along the wall (TO13, >600 ka) (Figure 6D), on which a younger honey-coloured subaqueous speleothem has grown (TO14, 577.2 ±60.6 ka) (Figure 6D), which in turn corresponds to the older generation of the mushroom stipes (not sampled) and hats (TO15, 541.4 ±105.5 ka) (Figure 6E) (Table 3).

Proceeding deeper into the cave, the horizontal passage opens up into a large descending room (Pantheon), which lower part is covered with calcite crystals (Figure 6G). The room is decorated with large stalagmites and stalactites, all showing a white and powdery corroded surface towards the interior of the cave and deposition of reddish fines (toward the entrance) on the other side. The warm and wet air flowing from inside the cave toward the entrance causes this corrosion. This

397 airflow is forced to pass a narrower passage, and this compression causes condensation on the
398 speleothem sides facing toward the Pantheon below. The reddish powdery coating on the other side
399 was probably produced during the excavation works in the passage immediately beyond. Here the
400 cave turns from its original NE-SE direction in an E-W one for a few tens of metres, then turning
401 again back to the SW to develop along a fracture parallel to the one that guided the first 200 m of
402 the cave. In the narrower part connecting both fractures, underneath a calcite floor (TO16a, 581.3
403 ±143.3 ka), an older sand layer showing progradation toward Pantheon testifies to the ancient flow
404 direction (toward the NE) (Figure 6F). These sands (TO16b), unfortunately, have not been dated;
405 however, the above lying TO16a calcite belong to the same generation as the subaqueous TO14-15
406 calcites. A few metres further in the SW direction, the roof is sculpted with a chain of
407 interpenetrating rising cupolas, forming a giant rising channel feature, indicating again rising flow
408 from SW to NE (Figure 6H). Less than 10 m away, there is another deep shaft, Pozzo dell'Ade, on
409 the bottom of which a narrow fracture-guided passage continues to the east. This area is intensely
410 covered with recent calcite and aragonite bushes and crystals, making it one of the most delicate
411 cave areas. The combination of all above mentioned observations is compatible with Pozzo
412 dell'Ade acting as the main source of upwelling of deep water and thus can be considered as a
413 major feeder of the original cave system. Another fracture-controlled shaft is present 30 m further
414 to the SW, but has not been investigated (to avoid the damage to the delicate speleothems covering
415 walls and floor). This might be another feeder. Except some small active epigene drippings, no
416 other source of concentrate flow to the system has been detected. From here, the cave continues in a
417 NE-SW direction, and 20 m from this shaft the artificial tunnel connecting to Bàsura Cave is
418 reached. Continuing to the SW a tunnel, half-excavated, continues and allows to enter a smaller
419 passage (Ramo dei Cristalli), where floor, walls and roof are almost entirely covered with delicate
420 aragonite and calcite bushes and needles (Figure 6I), as well as minerals such as hydromagnesite,
421 dolomite and magnesite (T5-6); this testifies the high Mg-content of the host rock (black
422 dolostones) and local evaporative conditions allowing oversaturation and crystallization of such

mineral species (Table 1). The roof of these passages is often corroded up to the underlying weathered host rock by channelised flows of warm and moist air that condenses and partially dissolves the rock, hollows condensation channels, displaying as soft red-brown counter-relief weathered surfaces (Figure 6I). Analyses of this several centimetres thick weathering material (T7-T11) have shown the presence of hematite, muscovite, illite, and quartz (Table 1).

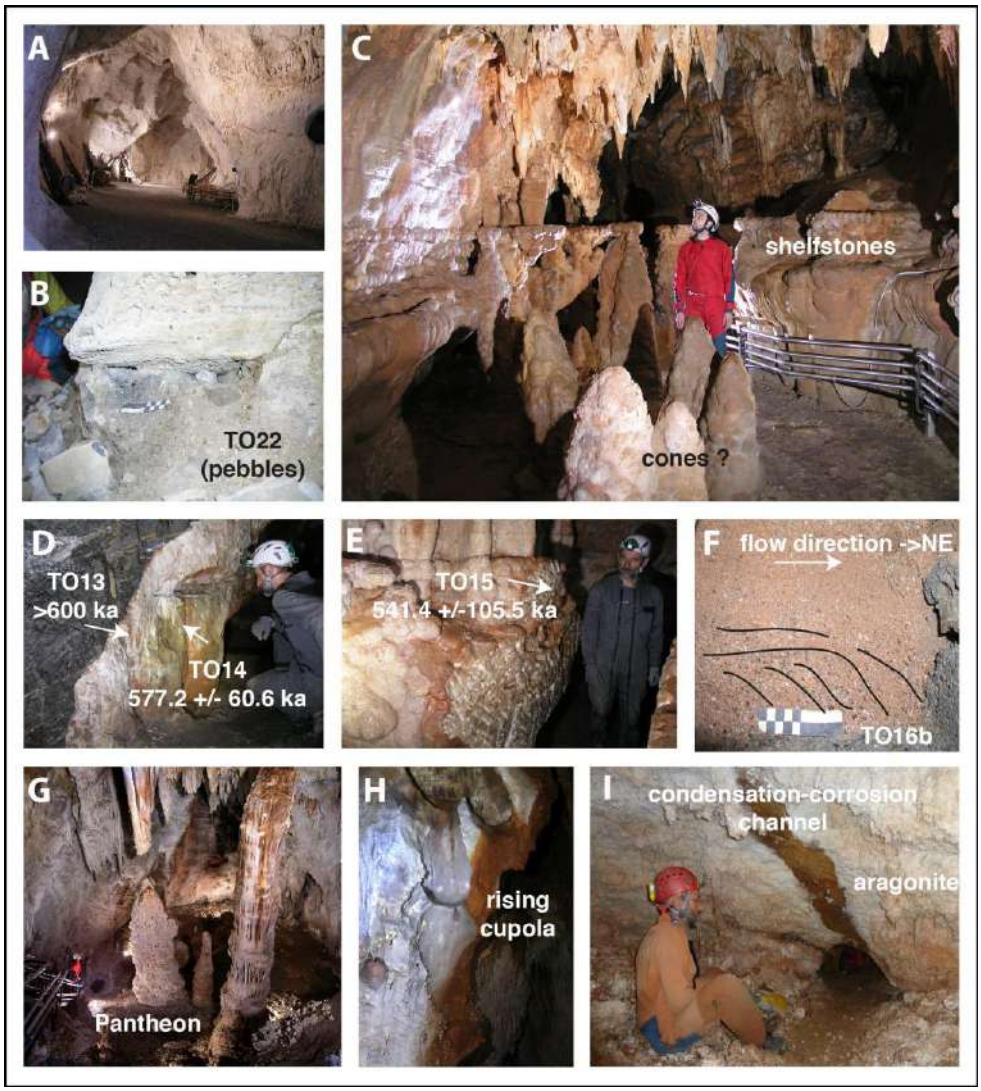

Figure 6 – Morphologies and deposits in Lower Santa Lucia Cave (Photos by Jean-Yves Bigot): A. The large Tanone gallery following the entrance displays walls with weathered rocky surfaces and very sparse remnants of corroded flowstones.; B. The fluvial pebble deposit (TO22) in Tanone gallery, not far from the entrance; C. Capitelli, with the raft cones (?) in the foreground, and the different levels of shelfstone forming the mushroom-like speleothems; D. The end of the artificial

tunnel dug in dark dolomite with white veins (left), opens in Capitelli, where white mammillary (subaqueous) calcite (TO13) is covered with a younger brownish calcite (TO14) representing a flowstone or shelfstone (subaerial); E. The top shelfstone of the mushroom-like speleothems (TO15), representing the youngest generation of TO14; F. Gravel deposit (TO16b) just below the Pantheon, underlying a dated flowstone level (TO16a); interpretation of progradation structure shows a paleo-flow toward the NE; G. The nice Pantheon room, flow welled up from the hole below the person; H. The chain of rising cupola between Pozzo dell'Ade and Pantheon also showing flow toward NE; I. The narrower passages in Crystal Gallery (or Ramo dei Cristalli) are entirely covered with aragonite and other white minerals, cut by a clear condensation-corrosion channel on the roof, where rock is deeply weathered (Photo by Philippe Audra).

4.1.4. Bàsura Cave

Bàsura Cave opens at an altitude of 186 m asl. It has two entrances less than 10 m apart, the higher one developed on the same bedding plane and a few metres higher than the main one (Figure 3D). Both, although developed along a bedding plane parting, are perfectly circular (Figure 7A). Entering into the cave, the floor below the side walls is covered with angular cryoclastic elements showing an infill from external slope material. These sediments rapidly disappear leaving place only to fine sediments. The cave penetrated 10 m more inside the mountain until a narrow passage between a flowstone and the roof impeded people to pass. This is the point where locals opened the passage in 1953, leading to the discovery of most of the cave and the ancient-men footprints. U/Th dating of the top of this entrance flowstone reported an age of 12.34±0.16 ka (the base of the flowstone being 205±24 ka years old (Molleson *et al.*, 1972).

Once passed this narrow passage, now made comfortable by a short tunnel, the cave shows widespread speleothem deposition with very clear signs of corrosion, also affecting walls (widened corroded fractures, condensation-corrosion pits). The cave is a collection of large rooms and smaller conduits, with smooth walls, rising features, cupolas, widened fractures, rock fins, and impressive

speleothems. All is compatible with very slowly flowing water, lacking marks of turbulent flow such as scallops or allogenic coarse sediments. A large flowstone ascending toward the corridor of the footprints has been used to reveal short-lived geomagnetic excursions during the Brunhes Chron, and the deepest part of the dated drill core is older than 615 ka (but the rock below the flowstone has not been reached). The flowstone appears to have grown from the MIS13 (over 500 ka) to the beginning of MIS7 (around 240 ka) (Pozzi *et al.*, 2019).

In the corridor of the footprints (the main passage in the entire karst system following a bedding plane parting), several speleothems show a more important corrosion, especially in the vicinity of side branches (Fascio, Small Lakes). These narrow side branches descend to lower parts of the cave, and show many signs of rising flow. In a small alcove in the Fascio Branch, a brown crust has been sampled (TO21), corresponding to a bat guano by-product (F- or OH-apatite, with detrital contamination of quartz and mica). In the branch named “Small Lakes”, a narrow passage leads to some small, now-dry pools. A sample of mammillary calcite (TO20) has given an age of 35.0 ± 0.3 ka, so rather recent (Table 3). Three of these smaller ascending lower passages are most probably ancient feeders of the original cave system (Figure 3D).

Proceeding in the cave, the passage is occupied by a lake, formed by more recent infiltrating water, and the cave floor is characterised by the only sign of temporary water flow in the cave. A large rimstone dam is broken and has blocked the transport of large cave bear bones from east to west following the local slope (the bones are all accumulated on the eastern side of the rimstone dam). From here on, going east, the floor of the cave is effectively a riverbed, and the related fluvial sediments are mainly composed of clay with numerous cave bear bones and skulls. This deposit leads to the Mystery Room, where the signs of prehistoric footprints come to an end. The bones and skulls of cave bears probably came from a higher passage, still visible today but closed by a flowstone, likely leading to unknown chambers where cave bears used to hibernate (in Bàsura Cave there are no signs of cave bear dens).

From Mystery Room, the cave becomes narrower and starts descending (Figure 7B); in the lower segments, white subaqueous well-developed speleothems indicate that this section has been underwater for a rather long period of time (Figure 7C). Before the opening of the cave (in the 50s), these parts of the cave were still underwater, but anthropic activities eventually drained the lake entirely. At the start of the steep descent towards “Cibele”, a sandy-gravel deposit in a red-brown matrix has been sampled (TO17), covered with a white calcite layer (TO18, >600 ka) (Figure 7D, Table 3). This calcite/sand couple could be an analogous of the similar TO16 deposit, which has a symmetrical location in Pantheon slope of Lower Santa Lucia, and which calcite is also >600 ka. Further down, the passage is characterised by up to 5 metre-tall “pool fingers” (microbial filaments gradually thickened by subaqueous mammillary calcite coating), and the presence of old calcite rafts, which are now up to a centimetre thick (Figure 7E). On the bottom of Cibele, nearby the artificial tunnel connecting to Lower Santa Lucia Cave, at the base of the thick subaqueous calcite filling, a pocket filled with calcite rafts has been sampled (TO19), reporting an age of 562.2 ± 77.1 ka (Figure 7F; Table 3). It is highly probable that the downward continuing branch at the base of Cibele was another feeder of the original system.

Three samples of calcite rafts have been taken in Bàsura Cave: an active raft deposit in the lower parts of Fascio Branch (T2), and two thick rafts in the Cibele area, one on top (T4) and one at the lowest part (T3). All of these show a stable isotope content compatible with temperatures in the range of present climatic conditions (between 13 and 14°C, Table 2). Transmitted-light microscopy has revealed the presence of primary monophase fluid inclusions in sample TO19 (Figure 8). The inclusions show characteristic inverted edges, indicating their primary origin. Primary monophase fluid inclusions either appear isolated (Figure 8a) or are clustered in fluid inclusion assemblages (Figure 8b). No primary two-phase fluid inclusions were observed in this sample. The occurrence of only monophase liquid inclusions imply that mineral crystallization happened in a low-temperature (ambient) hydrothermal environment.

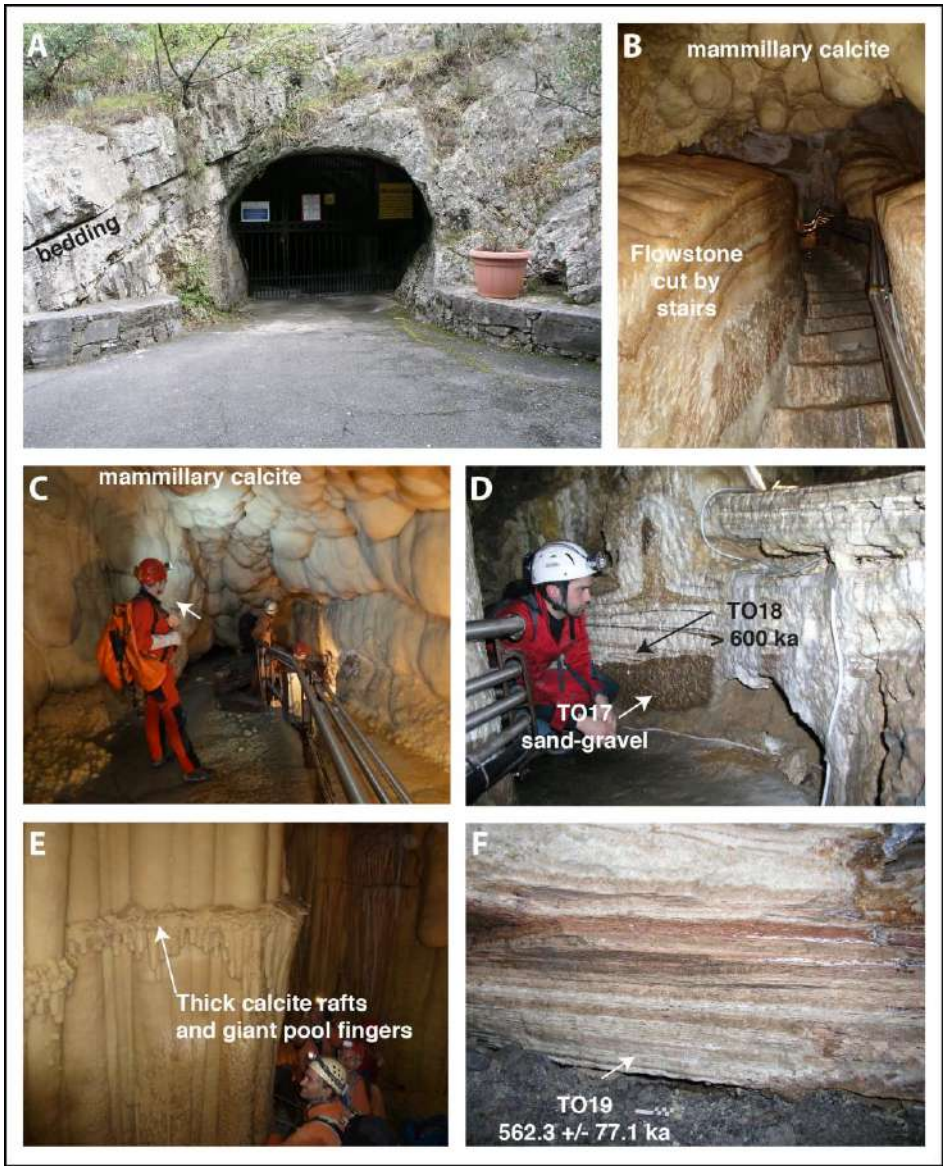

Figure 7 – Morphologies and deposits in Bàsura Cave (Photos by Jean-Yves Bigot (A-D-F) and Philippe Audra (B-C-E)): A. The rounded entrance of Bàsura cave showing no control by bedding planes; B. The steep descent towards Cibele, cut through the thick flowstone; C. The subaqueous mammillary calcite deposits of Cibele; D. The brownish sandy-gravelly deposits (TO17) below white calcite (TO17); E. The thick calcite rafts suspended upon a welt in the massive pool fingers covered with mammillary calcite; F. Subaqueous rafts sampled at the base of the Cibele rooms (TO19).

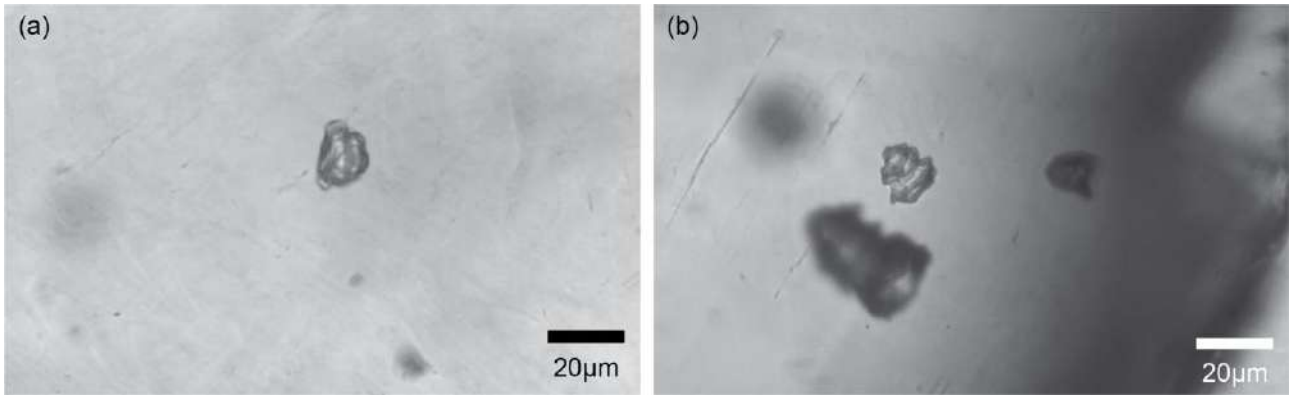

Figure 8 – Examples of primary all-liquid fluid inclusions in TO19 calcite (a, b). Fluid inclusions show characteristic inverted growth steps (b). Photomicrographs are the courtesy of Yves Krüger.

5. Discussion. Speleogenesis of Toirano karst system

5.1 Morphological indicators of speleogenesis

Although the original shape of the caves and their meso-morphologies have been greatly modified by later processes, several morphological observations in the different caves have shown a series of important speleogenetic indicators, which can be reassumed as follows:

1. The different remnants of the cave system are developed along clearly distinguishable levels, at altitudes of 340 (Ulivo), 250 (Colombo), 215 (Upper Santa Lucia), 210-205-200 (Lower Santa Lucia), and 185-175-165 m asl (Bàsura), respectively (Figure 9). These levels testify to relative long-lasting stable phases in which the local base level and caves were at the same altitude.

2. Morphologies related to fast and turbulent flow (scallops) have not been detected. Clastic sediments range from coarse pebbles to gravels, sands and clays. Apart from angular clasts located in entrances areas (especially Bàsura), which have been brought in by gravity or by solifluxion, the largest elements (pebbles) are located close to entrances with inward grain size decrease clearly pointing toward intrusions of allogenic fluvial material. This is also evidenced by their petrographic composition (quartzites, schists), as clearly shown in Colombo Cave. Cave passages have been entirely filled by these sediments, at least for the first 100-200 metres from the entrances. In the inner parts of the system, only smaller grain sizes are visible (gravels, sands), as long as they are not

concealed by later speleothem deposition. Samples TO16 and TO17 show a reworking of the allogenic material by internal flow toward outlets that maintained their activity during the infilling periods. Finally, fine sediments derive from a mixing of different sources, i.e. carbonates grains from disaggregation of the host rock, clays and iron oxides from insoluble material and red clay veins, and from allogenic fluvial sediments, as evidenced by typical minerals (quartz, mica, feldspars) trapped in the weathered material along the walls.

3. The caves are essentially characterised by morphologies due to slowly flowing waters, and it is clear from observations in several cave areas that these fluids followed ascending paths. These morphologies are rising channels, superposed cupolas and ceiling channels. Some ascending conduits are almost certainly feeders from which fluids rose. Except from limited seepage spots, no trace of significant epigenic recharge, either active or inactive, such as vadose shafts and meanders, have been detected. The recharge at the origin of the cave system is clearly hypogenic, *sensus* Klimchouk (2007), i.e. from below with no direct influence from immediate recharge areas on flow discharge and physical and chemical characteristics of the fluids.

4. Condensation-corrosion, both by convection of external warm and wet air masses, and vapours produced by bats and decay of guano deposits, have intensely modified walls and roofs morphologies in many portions of the caves, especially in the higher parts of the system that were not confined (Colombo, Upper and Lower Santa Lucia caves). This has made it difficult to recognise many of the typical morphologies of rising flow.

5. The active thermal and slightly sulphidic spring in the village of Toirano, only 500 m south of the caves and ~100 m below the Bàsura Cave, indicates ongoing processes of deep fluid circulation today. Analogously, deep fluid circulation might have been active in the past; hypogene fluids circulating in the carbonate rocks would have caused the formation of the karst network.

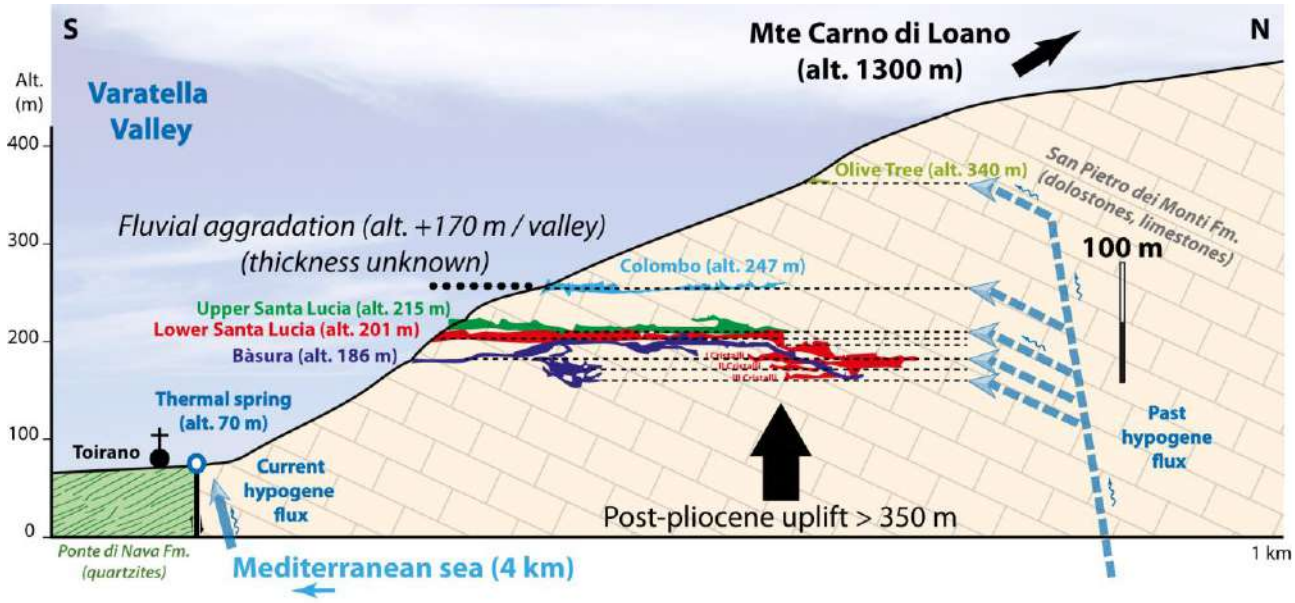

Figure 9 – – Schematic profile through Mt. Carmo showing the altitudinal distribution of the caves levels in relationship to their hypogene origin, to the uplifting and correlated Varatella valley deepening (Surveys courtesy of Gruppo Speleologico Cycnus e Delegazione Speleologica Ligure, 2001).

5.2. Hypogene origin of the system

The mineralogical analyses did not evidence the typical weathering by-products of sulfuric acid speleogenesis such as gypsum, alunite and jarosite (D'Angeli *et al.*, 2018). Instead, carbonate minerals abound, including calcite, aragonite, huntite, and magnesite (minerals typically found in dolostone-hosted caves), whereas gypsum, ardealite, brushite, F- and OH-apatite, leucophosphite/spheniscidite, and newberyite have been found on the old guano deposits (Audra *et al.*, 2019, Table 1).

The caves formed inside the carbonate rock mass without a direct connection to the surface, and before the Varatella torrent started carving its deep valley. Possibly thermal fluids rose along deep-rooted sub-vertical faults concentrating their corrosive action close to the water table, where the dissolved CO_2 was able to escape into the above lying air-filled chambers. Most dissolution occurred close to the water-air interface, and in the aerate part of the caves because of

583 condensation-corrosion. The action of minor amounts of H_2S-enriched fluids is not to be excluded
584 entirely, based on the low sulphidic character of the spring still active today (25.4-37.0 mg L^{-1};
585 Calandri, 2001), although evidences of sulphuric acid speleogenesis have not been found. However,
586 the signs of sulphuric acid interaction with the host rock, both weathering products (gypsum and
587 other sulphates) and typical corrosion morphologies (e.g., replacement pockets), could have been
588 easily weathered by the intense and long-lasting condensation-corrosion processes, and by the
589 recent action of infiltration waters. It is more likely that the cave-forming fluids were rich in CO_2,
590 and might have been slightly thermal, whereas sulphate (and sulphuric acid) played only a very
591 minor role (if at all). We claim that the Toirano caves are of hypogenic origin, with the earliest
592 speleogenesis governed by the upwelling of possibly low thermal fluids rich in CO_2.
593
594 Preliminary stable isotope analyses on the calcites of the *Antro di Cibele*, however, have pointed to
595 palaeo-temperatures in average of 13-14 °C. Such values are several centigrade lower than the
596 current temperature range found at the active thermal spring of Toirano (22-23°C), however similar
597 to the present climate in the valley (Toirano city 14.3 °C). The older calcite deposits show
598 temperatures ranging between 13 and 16 °C, similar to that of the Cibele calcite rafts. Recent (35
599 ka) mammillary calcite of "Small Lakes" are slightly colder (10 °C), possibly recording the cold
600 period conditions. Active rafts reveal a temperature of 14 °C, which is close to the current cave
601 temperature and mean annual average, and lower than the thermal spring temperature. The presence
602 of all-liquid primary fluid inclusions in one of the calcite rafts from the Cibele area also suggests
603 that the mineral depositing fluids were characterized by temperatures lower than ~50°C. We
604 suggest that all cave calcite deposited either from low-thermal water mixed with cold meteoric
605 seepage water, or directly from infiltrating waters. The $\delta^{13}C$ values (between -8 and -11‰) are
606 consistent with a contribution from above lying soils rather than hypogene flux (McDermott, 2004).
607 This is confirmed also by the $\delta^{18}O$ values which are typical of low temperature calcites precipitating
608 from mid-latitude precipitation waters.

609 Most of the calcite speleothems visually appearing as very old deposits reported ages beyond the U-
610 Th method limit (ca. 600,000 years), even in the lower (and possibly youngest) caves (Table 2). The
611 age of underground deposits can be used to constrain the minimal age of the cave (Columbu *et al.*,
612 2015; 2017). Consequently, the entire karst system and even the lower caves are certainly older than
613 600,000 years. Similar results were obtained by Bahain (1993), with the base of a flowstone in
614 Bàsura Cave showing inverse remanent magnetism (thus certainly older than 780 ka); ESR dates of
615 faunal remains in this basal sequence reported ages between 502 (±47) and 748 ka (±66), while
616 several U/Th dates resulted older than 557 ka (Shen, 1985). This is also confirmed by recent studies
617 in Bàsura Cave, where the bottom of a 2-metre-thick flowstone resulted older than 615 ka (Pozzi *et*
618 *al.*, 2019).
619 The allogenic sands sampled in Colombo Cave have delivered a burial age of approximatively 1.8
620 million years, which represents the minimum possible age of the voids these sands fill. These coarse
621 to fine sands have been carried into the caves during the Lower Pleistocene high stands. During the
622 Gelasian (ca. 2.6-1.8 Ma) the sea level (which greatly controlled the base level for the studied
623 caves) oscillated globally between -100 and +10 m with respect to present sea level (Rohling *et al.*,
624 2014). Taking 1.8 million years as a minimum age for the caves, Colombo Cave, since its
625 formation, would have been uplifted from that ancient sea level (-45 ± 55 m with respect to present
626 sea level) up to its current altitude (250 m asl), for a total uplift of 295 ± 55 m. This would deliver a
627 mean uplift rate of the portion of rocks north of the main fault (on which the thermal spring is
628 located) of the same amount in 1.8 Ma, corresponding to 0.16 ± 0.03 mm y^{-1}. This uplift is slightly
629 overestimated (Colombo Cave is older than 1.8 Ma, so the real uplift rate is lower), since the cave
630 formed before the intrusion of the dated sands (possibly at the Pliocene termination/Early
631 Pleistocene). However, taking into account this estimation of long-term uplift value, and since all
632 horizontal cave levels have formed in periods of relative base level still stand (and thus stability of
633 the sea level), we can at least estimate that the age of all cave levels: Ulivo might have an age
634 around 2.4 ± 0.4 Ma, Colombo Cave would have formed around 1.85 ± 0.35 Ma, Upper Santa Lucia

635 Cave around 1.65 ± 0.35 Ma, Lower Santa Lucia around 1.55 ± 0.35 Ma, and Bàsura Cave would
636 have formed around 1.45 ± 0.35 Ma (Table 5). Because hypogenic speleogenesis occurred before
637 the injection of alluvial sediments, the ages of the caves are most probably closer to the oldest
638 obtained estimates. This places the speleogenesis of the Toirano cave system during the Gelasian
639 and Lower Calabrian, and probably at the very end of Pliocene for the highest Ulivo. The presence
640 of a Messinian canyon offshore, and Pliocene Gilbert-delta deposits onshore in the vicinity of the
641 current coastline, evidence that the valley significantly entrenched during the Messinian Deep-sea-
642 level, then was refilled during the Pliocene by sediments sourced from the ongoing uplifted
643 mountain where strong erosion occurred. The discontinuous uplift of the study area mainly took
644 place during the Late Pliocene-Early Pleistocene, with marine Lower Pliocene sediments now
645 located at altitudes of up to 400 m asl (Carobene and Firpo, 2002; Ferraris *et al.*, 2012). Then,
646 following the Pleistocene uplift, a gradual entrenchment of the Varatella gorge occurred, with the
647 removal of most of the Pliocene marine deposits and Pleistocene terraces. The old fluvial material,
648 located above 100 m asl, has been only preserved in Toirano caves as intrusion material. They are
649 possibly related to 1) aggradation during Pleistocene, or 2) re-incision and injection in caves of the
650 reworked material. The cosmogenic burial age at about 1.8 Ma, if reliable, would point toward the
651 second option. Note that Colombo Cave predates this age, without indications on how much older
652 this cave could be with respect to the sediment intrusion. Regarding ages obtained from
653 speleothems U/Th dating, most are older than the method's limit (600 ka), making it difficult to
654 ascribe an age to the subaqueous deposits related to the initial phreatic stage. However, the partial
655 draining of the main pool stages (Capitelli in Lower Santa Lucia and Cibele in Bàsura, which are
656 located at the same elevation), probably still fed by minor hypogene recharge, is quite well
657 bracketed around 581-541 ka. Considering the age errors, this would correspond to a period
658 between ca. 720 and 440 ka (Table 3 and 5). The pool-stage record in the well-marked shelves of
659 Upper Santa Lucia is more recent (343 ±10 ka), even if the cave is located slightly higher. This
660 would indicate that portion of the main cave levels (USL-LSL-B, see table 3 for codes) were

underwater for approximately 400,000 years, comprised approximately between 720 and 330 ka. The age of dated stalagmites, which could have developed during or after this active hypogene pool stage, confirm the partial or complete draining as early as 400 ka. Flowstones older than 500 to 780 ka in Bàsura (Shen, 1985; Bahain 1993, Pozzi et al., 2019) suggest that some parts of the cave system were drained earlier.

Table 5 - Estimated ages of successive evolution of cave levels

Caves	**Alt. (m)**	**Proposed age of phreatic hypogene speleogenesis (Ma)** (deduced from uplift rates and age of oldest speleothems)	**Age pool speleothems and flowstones (ka)**	**Age stalagmites (ka)**
Ulivo	337	2.4 ± 0.4		
Colombo	247	1.85 ± 0.35 to > 0.6	> 600	376, 180
Upper Santa Lucia	215	1.65 ± 0.35 Ma	343	408
Lower Santa Lucia	201	1.55 ± 0.35 to > 0.6	581-541	
Bàsura	186	1.45 ± 0.35 Ma to > 0.6	562 - 35	
Thermal spring	70	Active		

5.3 Overprinting of late stage condensation-corrosion

5.3.1 Condensation-corrosion in the inner semi-confined parts of the cave system

Intense signs of condensation-corrosion are visible in the inner parts of the caves that were almost entirely confined before the artificial opening of the tunnel and calcite plugs, such as in the inner branches of Colombo Cave, in the (past) confined part of Lower Santa Lucia Cave, and especially in the Crystal Branches. Here, walls are covered by boxwork and deep-weathered soft material in between, with red-brown or greenish coloured surfaces (Figure 10A), whereas the dolomite host rock was originally black (Figure 6D). The weathered soft layer is several centimetres thick. It is mainly composed of loose carbonate grains with a high porosity (>25-30%), with minor amounts of iron oxy-hydroxides at the origin of the typical colour (hematite, goethite, Ti-magnetite) at the

origin of the typical colour, and detrital minerals (quartz, mica, feldspars, illite). Carbonates are provided by the disaggregation of the host rock, detrital mineral are remnants of old sediment filling of fluvial origin brought from external sources, and iron oxy-hydroxides originated either from host rock veins of red clay, or from the weathering of the detrital minerals.

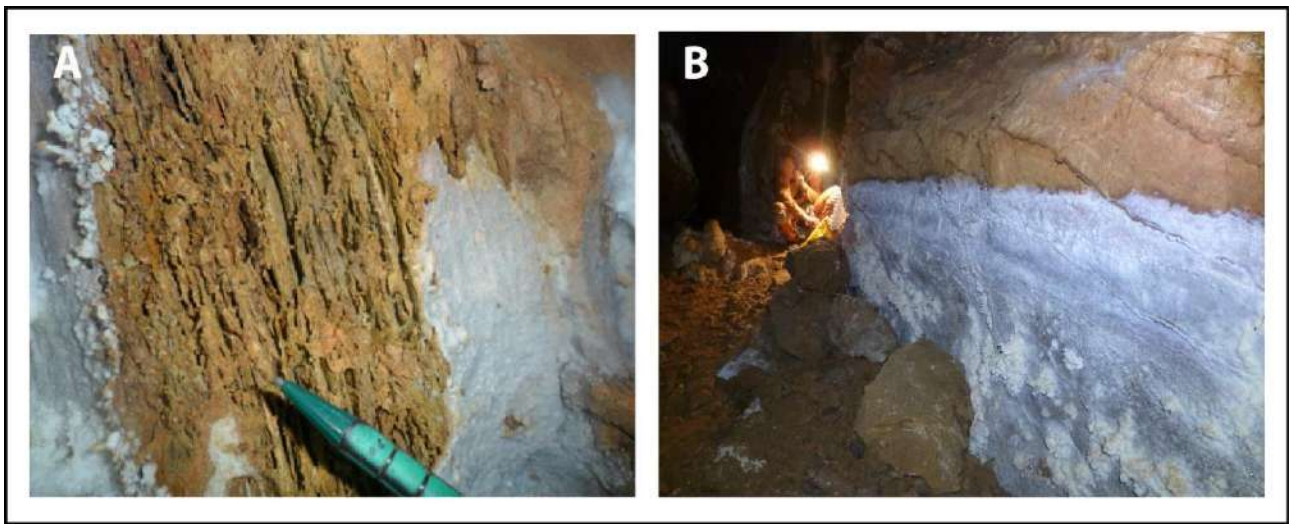

Figure 10 – Condensation-corrosion evidences: A. The black dolomite rock is deeply weathered by condensation-corrosion, making boxwork and soft residual material. Note the coating of evaporite minerals (calcite, aragonite, huntite, and hydromagnesite) (Photo by Jo De Waele); B. Air mass stratification in Crystals Branch produces a sharp limit between areas of evaporation-precipitation downward and condensation-corrosion in the upper parts (Photo by Philippe Audra)

Many places in these confined parts are covered by a secondary carbonate coating, composed of minerals that are typically found in caves hosted in dolostones (calcite, aragonite, huntite, and hydromagnesite). This coating is present in the lower parts of the passages (lower walls and floor), whereas the upper parts generally display boxwork and weathered layers (Figure 10B). Both are closely associated. In cave atmosphere close to moisture saturation, the subtle air convections allow air mass stratification and exchange, with condensation of warm and moist airflow on the cooler ceiling and evaporation in the cooler air flow along the warmer floor. Condensation produces

699 corrosion on the ceiling and a weathered layer, whereas evaporation produces crystallization in the
700 lower parts. The solutes produced by condensation-corrosion in the higher part of the passages
701 descend by gravity and are also attracted downward by capillary movements toward areas of
702 evaporation, where mineral precipitation can occur. The subtle airflow, currently present in Crystal
703 Branch, which is directed toward the external cliff, clearly shows a still active process. Here a
704 recent corrosion channel carves the white speleothem coating and the bedrock along the roof of the
705 passage (Figure 6I). However, such slow process requires long time spans to produce such deep
706 weathered layers. It possibly started after the early stages when hypogene caves began draining, but
707 when low-thermal water was still present at depth, or at least the rock mass was still heated by the
708 thermal fluids, producing rising warm and moist air flows. These processes clearly postdate the
709 initial phreatic hypogene stage, which would have washed away the soft weathered material. Since
710 many speleothems are older than 600 ka (Table 3) and some even older than 780 ka, one can expect
711 that the condensation-corrosion process in confined areas occurred from about at least 1 Ma. The
712 successive openings to the surface of some entrance parts drastically changed these semi-confined
713 conditions, starting much more active condensation-corrosion processes.
714
715 **5.3.2. Condensation-corrosion and biocorrosion in the large entrance parts**
716 Condensation-corrosion is particularly evident in the large passages of Colombo, in both Upper and
717 Lower Santa Lucia caves, and in Bàsura Cave. Importantly, the caves are located on a southwest
718 facing cliff, where warm and wet air masses from the sea frequently rise along the valley and cause
719 the formation of coastal fogs. During summers, the air masses coming from the sea have average
720 temperatures well above 20°C, able to produce condensation on the cave walls that are around
721 15°C, or even colder. Furthermore, efficient air circulation prevents the cave atmosphere to warm
722 up because of the release of condensation latent heat, keeping the cave walls colder than the
723 entering air, and thus sustaining a continuous production of condensation waters. In the lower parts
724 of the cave passages, dripping condensation waters, containing dissolved carbonates, fall to the

ground and evaporate, causing the deposition of new microcrystalline calcite that is mostly removed by airflow. The highly undersaturated condensation waters have produced the weathering (partial dissolution) of the rock walls causing their powdery appearance.

In Lower Santa Lucia, the entrance passage (Tanone) is intensely corroded by condensation, mainly due to its large entrance allowing warm and moist air to circulate freely into the cave. Most of the flowstones have disappeared, except in sheltered corners (Figure 6B). Here, remnants of coarse pebbles cemented by an old flowstone show that the passage has been entirely cleaned from its fluvial filling. It now displays as a large tunnel, with smooth wavy walls and a light colour due to the thin dry weathering layer (Figure 6A). Compared to the passage size beyond the calcite plug isolating the Capitelli from Tanone, it clearly appears that Tanone "tunnel" significantly expanded by condensation-corrosion, probably for several metres, cancelling most of its original features and sediments.

In Bàsura cave, condensation-corrosion morphologies are also clearly visible: i) at the entrances, where the initially elliptical phreatic conduits along the bedding plane have been subsequently rounded (Figure 7A); ii) immediately behind the small passage that was opened in 1953; iii) on walls and speleothems intensely corroded by airflow. Here condensation is possibly related to the variations in pressure of the airflow, when the passage was still closed, and airflow was subdued to important pressure variations. This is confirmed by the fact that the signs of corrosion are most evident in the first ten metres from the (originally) narrow passage. In the Footprints Passage, several speleothems are deeply corroded by airflows. Here, condensation is probably caused by the formation of a mixing cloud (Badino, 2010), since air convection from lower branches (Fascio, Small Lakes) mixes with air masses in this part of the cave. In addition, widened corroded fractures and condensation-corrosion pits, which are strongly developed, testify the intense activity of the process in this area.

The condensation-corrosion process is also boosted by bat colonies, which abundant presence in the past is testified by the large old guano and phosphate deposits. Phosphate deposits as crusts on

751 carbonate walls and calcite speleothems mainly consist in F- and OH-apatite, in
752 leucophosphite/spheniscidite in presence of clastic material, whereas more recent and still decaying
753 guano is covered by sulphates and phosphates such as gypsum, ardealite, brushite, and newberyite
754 (Table 1; Audra *et al.*, 2019). Guano decay is an exothermic process releasing both water vapour
755 and carbon dioxide, thus enhancing condensation above the guano heaps, and high CO_2 levels in the
756 air. Other acids released by guano decay make the atmosphere particularly aggressive and
757 corrosive. In addition, bat exhalations add considerable amounts of heat, vapour, and carbon
758 dioxide. All these aggressive solutions combine and are responsible of the biocorrosion of cave
759 floor, walls, and ceiling, where bio-cupolas are the most expressive features (Lundberg and
760 McFarlane, 2009, 2012, 2015; Audra *et al.*, 2016; Dandurand *et al.*, 2019).
761 This powerful process can explain the exceptionally wide central room in Colombo Cave, where a
762 central biconcave rock pillar is the leftover of intense condensation-corrosion (Figure 4F). The
763 same is testified by the presence of old corroded flowstones, as well as typical morphologies such
764 as cupolas and the wavy (mega-cusped) appearance of the cave walls. Additionally, the pebbles that
765 were introduced into the cave, and that probably entirely filled it, have completely disappeared,
766 leaving only some patches of conglomerates in sheltered niches. Last but not least, the scarcity of
767 graffiti remnants shows the ongoing activity of corrosion processes. Based on our observations, the
768 wall retreat by biocorrosion processes alone can here be estimated in at least 1 m on both sides of
769 the passage, probably double on the roof.
770 In Upper Santa Lucia Cave, masses of old guano are still visible. Biocorrosion features are intensely
771 developed. Interpenetrating cupolas are carving the chamber ceilings, cutting both rock and old
772 calcite speleothems (Figure 5D). Dripping pots are developing on the vertical of ceiling pendants
773 that concentrate condensation runoff (Figure 5E). However, on the contrary to Colombo Cave,
774 biocorrosion processes seem to be subdued, as testified by the considerable amount of well-
775 preserved graffiti, even on top of cupolas that are the places of the most intense condensation
776 (Figure 5C). This could be explained by the continuous frequentation of the cave by pilgrims and by

777 the gating of the inner part (Figure 5A) that prevented intrusion of bats for centuries, and thus
778 preserved the historical traces of frequentation.
779
780 **6. Conclusions**
781 On the basis of the geomorphological observations, supported by geochemical analyses and U/Th
782 dating, the origin of these complex caves cannot be attributed to a "classical" epigenic vadose and
783 phreatic speleogenetic model only. The Bàsura-Santa Lucia-Colombo caves formed by the action of
784 rising hypogenic fluids that followed deeply-rooted subvertical fractures. The rising conduits
785 (*feeders*) are still visible in the lower levels of the cave system (Bàsura and Lower Santa Lucia
786 caves), whereas they are obliterated in the higher and older levels by abundant authigenic and
787 residual sediments. In the lower passages, the traces of ascending fluids are still well visible in
788 many areas, with rising channels and superimposed cupolas.
789 Based on the observations made in the highest of the studied caves (Colombo) the following
790 speleogenetic scheme can be presented (Figure 11): A) The cave started forming at the water table
791 level fed by a deep-rooted fracture, with thermal (possibly H_2S-rich) waters carving the cave in both
792 phreatic, but mainly aerate conditions; B) A marine ingression during the final phases of the
793 Pliocene and early Pleistocene caused the river valleys to aggrade and enlarge; the entrance of the
794 cave was completely filled with gravels and sands (pockets on the roof of the cave are still filled
795 with remnants of these sediments, which burial age is around 1.8 Ma); C) successive Pleistocene
796 uplift phases of the mountains caused the Varatella torrent to entrench, partially emptying the cave
797 which, at least in the early stages, was probably still actively enlarging by rising hypogene fluids.
798 The continuous uplift caused the intersection of the water table with the feeding fractures to shift
799 laterally and to lower elevations, causing the formation of the lower levels of the cave system; D) in
800 the final stages the cave system was abandoned by flowing hypogenic waters, and since then the
801 large cave entrances are subdued to air circulation, bat roosting and frequentation and condensation-

corrosion processes started to remove most remnants of the older sediments and speleothems (several of which are beyond the U/Th dating limit, i.e. > 600 ka).

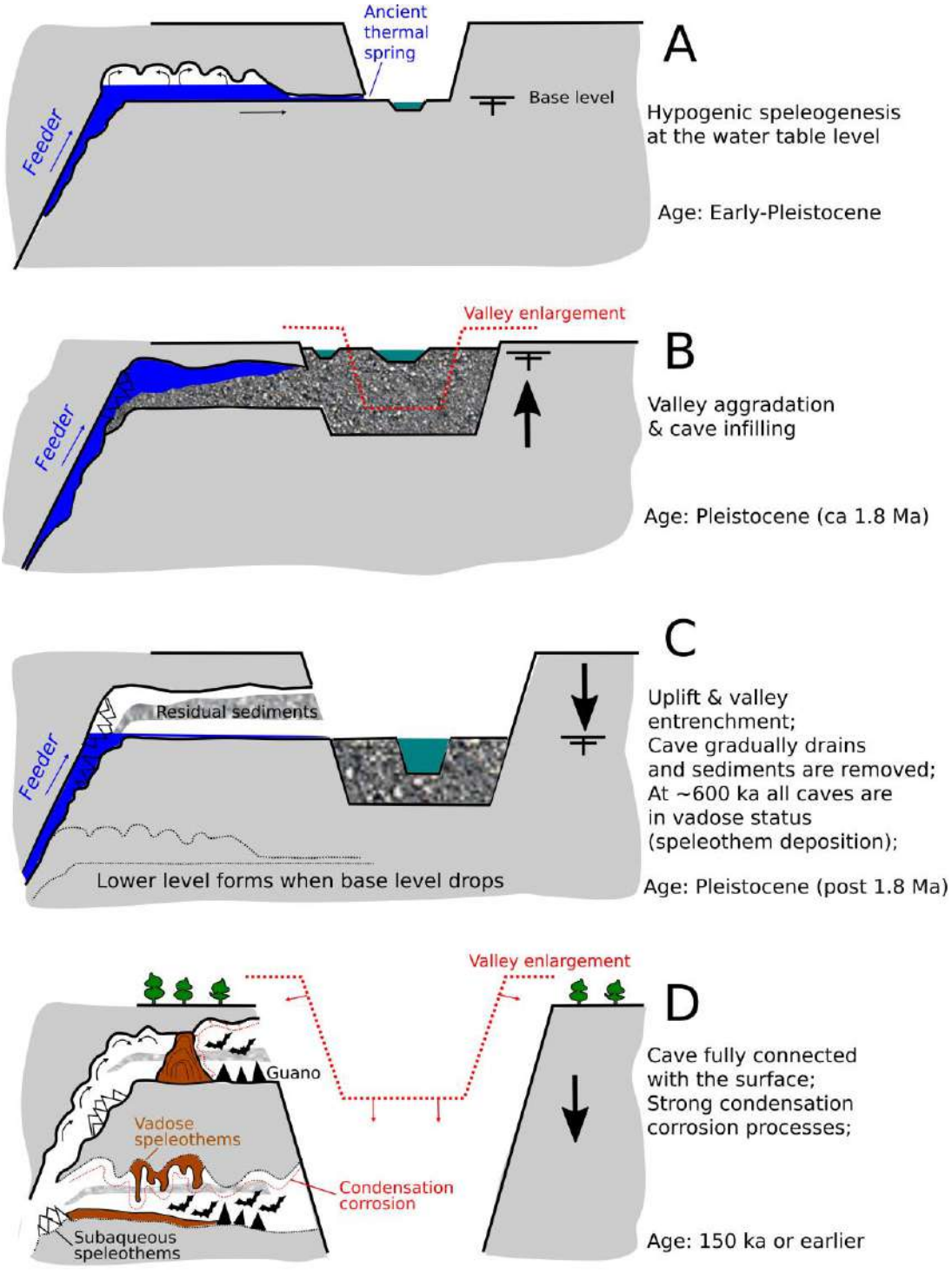

Figure 11 – Evolution of a given level of Toirano Caves (especially Colombo and Lower Santa Lucia). A. Horizontal cave connected to base level develops with hypogene upflow and condensation-corrosion in the confined part. B. Fluvial aggradation (Early Pleistocene) rises the

base level and fills the entrance passages with coarse fluvial material. C. Subsequent base level drop following the continuous uplift allows reopening of the cave with partial removing of the fluvial filling. D. Because of slope retreat occurs, condensation-corrosion occurs in the previously confined portions of the cave through geothermal effect, with intense effect in the entrance accessible to bat colonies.

Only in more recent times, at least 150 ka (on the basis of the oldest archaeological artefacts), but probably much earlier, the entire cave system fully connected with the external atmosphere, initiating the air circulation and local condensation-corrosion processes. All signs of vadose flow visible today are to be connected to recent invasion or interception of small inflows or infiltrations in the pre-existing hypogenic cave system.

The intense condensation-corrosion, still very active today, has erased many of the morphologies and deposits of the original hypogenic speleogenetic phase. Ancient guano deposits appear to have a strong influence on later vadose condensation-corrosion processes, playing an important role in shaping the voids they occupy. Wall retreat by sole condensation-corrosion can be estimated in over 1 metre in the highest caves (Colombo) due to their entrance size, exposure to moving external air mass directions, and past presence of large bat colonies. Condensation-corrosion, however, is also active in more recently opened caves such as Bàsura, and warrants attention in the future for conservational issues.

We suggest taking this study as a guideline for a thoroughly investigation of cave evolution, based on a correct interpretation of underground morphologies, sustained by geochemical analyses, anchored in time by dating and coherently integrated with surface events.

Acknowledgements

Many thanks to the staff of the Toirano Caves, and especially to Dr. Flavia Toso, local geologist interested in knowing more about the caves, to archaeologist Dr. Marta Zunino, Scientific Director

834 of Toirano Caves, for her availability, enthusiasm and continuous support, to Dr. Elisabetta
835 Starnini, of the University of Pisa, and to the Archaeological Superintendency of Liguria, the
836 Managing Authority of the show caves, and the Municipality of Toirano. Yves Krüger is thanked
837 for his help in fluid inclusion petrography.. ASTER AMS national facility (CEREGE, Aix-en-
838 Provence) is supported by the INSU/CNRS, the ANR through the "Projets thématiques
839 d'excellence" program for the "Equipements d'excellence" ASTER-CEREGE action and IRD".
840 U/Th dating was supported by grants from the Science Vanguard Research Program of the Ministry
841 of Science and Technology (MOST) (109-2123-M-002-001 to C.-C.S.), the National Taiwan
842 University (109L8926 to C.-C.S.), the Higher Education Sprout Project of the Ministry of
843 Education, Taiwan ROC (109L901001 to C.-C.S.).
844

845 **References**

846 Arobba D, Boschian G, Caramiello R, Giampietri A, Negrino F, Tozzi C. 2008. La grotta del
847 Colombo : indagini geoarcheologiche, palinologiche e sull'industria litica. *Toirano e la Grotta*
848 *della Bàsura. Atti del Convegno, Bordighera*, 69-88.
849 Audra P, Palmer AN. 2016. Research frontiers in speleogenesis. Dominant processes,
850 hydrogeological conditions and resulting cave patterns. *Acta Carsologica* **44**: 315-348.
851 Audra P, Barriquand L, Bigot J-Y, Cailhol D, Caillaud H, Vanara N, Nobécourt J-C, Madonia G,
852 Vattano M, Renda M. 2016. L'impact méconnu des chauves-souris et du guano dans
853 l'évolution morphologique tardive des cavernes. *Karstologia,* **68**: 1-20.
854 Audra P, De Waele J, Bentaleb I, Chroňáková A, Krištůfek V, D'Angeli IM, Carbone C, Madonia
855 G, Vattano M, Scopelliti G, Cailhol D, Vanara N, Temovski M, Bigot J-Y, Nobécourt J-C, Galli
856 E, Rull F, Cailhol D. 2019. Guano-related phosphate-rich minerals in European
857 caves. *International Journal of Speleology* **48**: 75-105.
858 Badino G. 2010. Underground meteorology-"What's the weather underground?". *Acta*
859 *Carsologica* **39**: 427-448.

860 Bahain J-J. 1993. *Datation par résonance de spin électronique (ESR) de carbonates et d'émail*
861 *dentaire quaternaires - Potentiel et limites*. Thesis. Muséum National d'Histoire Naturelle, Paris,
862 114 p.
863 Bella P, Bosák P, Braucher R, Pruner P, Hercman H, Minár J, Veselsky M, Holec J, Léanni L.
864 2019. Multi-level Domica–Baradla cave system (Slovakia, Hungary): Middle Pliocene–
865 Pleistocene evolution and implications for the denudation chronology of the Western
866 Carpathians. *Geomorphology* **327**: 62-79.
867 Boni A, Cerro A, Gianotti R, Vanossi M. 1971. Note illustrative carta geologica d'Italia. Foglio 92-
868 93. Albenga – Savona. Servizio Geologico d'Italia: Roma.
869 Cailhol D, Audra P, Nehme C, Nader FH, Garašić M, Heresanu V, Gucel S, Charalambidou I,
870 Satterfield L, Cheng H, Edwards RL. 2019. The contribution of condensation-corrosion in the
871 morphological evolution of caves in semi-arid regions: preliminary investigations in the Kyrenia
872 Range, Cyprus. *Acta Carsologica* **48**: 5-27.
873 Calandri G. 2001. L'evoluzione del carsismo nel Toiranese: nota preliminare. In *Atti V Convegno*
874 *Speleologico Ligure "Toirano 2000"*. Toirano, Italy; 117-120.
875 Cauche D. 2007. Les cultures moustériennes en Ligurie italienne : analyse du matériel lithique de
876 trois sites en grotte. *L'anthropologie*, **111**: 254–289. doi:10.1016/j.anthro.2007.05.002
877 Calvet, M, Gunnell, Y, Braucher, R, Hez, G, Bourlès, D, Guillou, V, Delmas, M, ASTER Team.
878 2015. Cave levels as proxies for measuring post-orogenic uplift: Evidence from cosmogenic
879 dating of alluvium-filled caves in the French Pyrenees. *Geomorphology* **246**: 617-633.
880 Carobene, L, Firpo, M. 2002. Forme terrazzate relitte di genesi marina lungo la costa ligure tra
881 Genova e Savona (Liguria Occidentale). *Il Quaternario* **15**: 53-68.
882 Cavallo C. 1990 - *Indagine idrogeologica su alcune sorgenti del Toiranese*. 160 p. PhD thesis,
883 Univ. of Genova.
884 Cavallo C. 2001. Geologia e carsismo del massiccio del Monte Carmo di Loano. *Atti V Convegno*
885 *Speleologico Ligure "Toirano 2000"*. Toirano, Italy; 17-21.

886 Chiesa R. 2007. La Grotta del Colombo di Toirano (SV): Contributo preliminare alla conoscenza
887 della cavità. In *Atti XX Congresso Nazionale di Speleologia*. Iglesias, Italy. *Memorie dell'Istituto*
888 *Italiano di Speleologia* 2 (**21**): 130-138
889 Citton P, Romano M, Salvador I, Avanzini M. 2017. Reviewing the upper Pleistocene human
890 footprints from the 'Sala dei Misteri' in the Grotta della Bàsura (Toirano, northern Italy) cave:
891 An integrated morphometric and morpho-classificatory approach. *Quaternary Science*
892 *Reviews* **169**: 50-64.
893 Clauzon G, Rubino J-L, Suc J-P. 1996. *Les rias pliocènes du Var et de Ligurie: comblement*
894 *sédimentaire et évolution géodynamique*. Excursion commune Groupe français de
895 géomorphologie et Groupe français d'étude du Néogène, 109 p.
896 Columbu A, De Waele J, Forti P, Montagna P, Picotti V, Pons-Branchu E, Hellstrom J, Bajo P,
897 Drysdale R. 2015. Gypsum caves as indicators of climate-driven river incision and aggradation
898 in a rapidly uplifting region. *Geology* **43**: 539-542.
899 Columbu A, Chiarini V, De Waele J, Drysdale R, Woodhead J, Hellstrom J, Forti P. 2017. Late
900 quaternary speleogenesis and landscape evolution in the northern Apennine evaporite areas.
901 *Earth Surface Processes and Landforms* **42**: 1447-1459.
902 Columbu A, Spötl C, De Waele J, Yu TL, Shen C C, Gázquez F. 2019. A long record of MIS 7 and
903 MIS 5 climate and environment from a western Mediterranean speleothem (SW Sardinia,
904 Italy). *Quaternary Science Reviews* **220**: 230-243.
905 Columbu A, Chiarini V, Spötl C, Benazzi S, Hellstrom J, Cheng H, De Waele J. 2020. Speleothem
906 record attests to stable environmental conditions during Neanderthal-Modern Human turnover in
907 Southern Italy. *Nature Ecology & Evolution* **4**: 1188-1195.
908 Dandurand G, Duranthon F, Jarry M, Stratford DJ, Bruxelles L. 2019. Biogenic corrosion caused by
909 bats in Drotsky's Cave (the Gcwihaba Hills, NW Botswana). *Geomorphology* **327**: 284-296.

910 D'Angeli IM, Carbone C, Nagostinis M, Parise M, Vattano M, Madonia G, De Waele J. 2018. New
911 insights on secondary minerals from Italian sulfuric acid caves. *International Journal of*
912 *Speleology* **47**: 271-291.
913 D'Angeli, IM, Nagostinis, M, Carbone, C, Bernasconi, SM, Polyak, VJ, Peters, L, McIntosh, B, De
914 Waele, J. 2019. Sulfuric acid speleogenesis in the Majella Massif (Abruzzo, Central Apennines,
915 Italy). *Geomorphology* **333**: 167-179.
916 De Lumley H, Giacobini G, Vicino G, Yokoyama Y. 1984. New data concerning the dating and
917 interpretation of human footprints present in the **"**grotta della Bàsura**"** at Toirano (Savona,
918 northern Italy). Results of an international round table. *Journal of Human Evolution* **13**: 537-540.
919 De Waele J, Plan L, Audra P. 2009. Recent developments in surface and subsurface karst
920 geomorphology: An introduction. *Geomorphology* **106**: 1-8.
921 De Waele, J, Audra, P, Madonia, G, Vattano, M, Plan, L, D'Angeli, IM, Bigot, JY, Nobécourt, JC.
922 2016. Sulfuric acid speleogenesis (SAS) close to the water table: examples from southern
923 France, Austria, and Sicily. *Geomorphology* **253**: 452-467.
924 De Waele J, D'Angeli IM, Bontognali T, Tuccimei P, Scholz D, Jochum KP, Columbu A,
925 Bernasconi SM, Fornós JJ, González ERG. 2018 Speleothems in a north Cuban cave register sea
926 level changes and Pleistocene uplift rates. *Earth Surface Processes and Landforms* **43**: 2313-
927 2326.
928 Fanucci F. 1985. La Grotta preistorica della Bàsura. *Rivista di Studi Liguri* **51**: 341-343.
929 Fanucci F, Firpo M, Ramella A. 1987. Genesi ed evoluzione di piane costiere del Mediterraneo:
930 esempi di piccole piane della Liguria. *Geografia Fisica e Dinamica Quaternaria*, **10**: 193-203.
931 Ferraris F, Firpo M, Pazzaglia FJ. 2012. DEM analyses and morphotectonic interpretation: The
932 Plio-Quaternary evolution of the eastern Ligurian Alps, Italy. *Geomorphology* 149: 27-40.
933 Ford D, Williams P. 2007. Karst Hydrogeology and Geomorphology. John Wiley & Sons:
934 Chichester.

935 Gázquez F, Columbu A, De Waele J, Breitenbach SF, Huang CR, Shen CC, Lu Y, Calaforra J-C,
936 Mleneck-Vautravers MJ, Hodell DA. 2018. Quantification of paleo-aquifer changes using
937 clumped isotopes in subaqueous carbonate speleothems. *Chemical Geology* **493**: 246-257.
938 Gruppo Speleologico Cycnus & Delegazione Speleologica Ligure. 2001. Speleologia e carsismo del
939 Toiranese". *Atti V Convegno Speleologico Ligure "Toirano 2000"*. Toirano, Italy.
940 Klimchouk A. 2007. Hypogene speleogenesis: hydrogeological and morphogenetic Perspective. –
941 National Cave and Karst Research Institute, Special Paper **1**, 106 pp.
942 Krüger, Y, Marti, D, Staub, RH, Fleitmann, D, Frenz, M. 2011. Liquid–vapour homogenisation of
943 fluid inclusions in stalagmites: Evaluation of a new thermometer for palaeoclimate
944 research. *Chemical Geology* **289**: 39-47.
945 Leél-Őssy, S. 2017. Caves of the Buda Thermal karst. In Klimchouk A, Palmer, AN, De Waele, J,
946 Auler, AS, Audra, P. (Eds.) Hypogene Karst Regions and Caves of the World, Cave and Karst
947 Systems of the World. Springer, Cham. https://doi.org/10.1007/978-3-319-53348-3_18
948 Lundberg J, McFarlane DA. 2009. Bats and bell holes: the microclimatic impact of bat roosting,
949 using a case study from Runaway Bay Caves, Jamaica. *Geomorphology* **106**: 78-85
950 http://dx.doi.org/10.1016/j.geomorph.2008.09.022.
951 Lundberg J, McFarlane DA. 2012. Post-speleogenetic biogenic modification of Gomantong Caves,
952 Sabah, Borneo. *Geomorphology* **157-158**: 153-168.
953 https://doi.org/10.1016/j.geomorph.2011.04.043
954 Lundberg J, McFarlane DA. 2015. Microclimate and niche constructionism in tropical bat caves: A
955 case study from Mount Elgon, Kenya. In Feinberg J, Gao Y & Alexander EC Jr. (Eds.). Caves and
956 Karst across Time, *Geological Society of America Special Paper*, G,
957 http://dx.doi.org/10.1130/2015.2516(18).
958 Marini M. 2004. *Carta geologica del Pliocene ligure di Albenga (Alpi Marittime – Provincia di*
959 *Savona), 1:25.000*. SELCA: Firenze.
960 McDermott F. 2004. Palaeo-climate reconstruction from stable isotope variations in speleothems: a
961 review. *Quaternary Science Reviews*, **23**: 901-918.

962 Menardi Noguera A. 1984. Nuove osservazioni sulla struttura del massiccio del Monte Carmo (Alpi
963 Liguri). *Bollettino della Società Geologica Italiana* **103**: 189-203.
964 Molleson TI, Oakley KP, Vogel JC. 1972. The antiquity of human footprints of Tana della Bàsura.
965 *Journal of Human Evolution* **1**: 467-471.
966 Morelli N. 1890. Nota sopra due caverne recentemente esplorate nel territorio di Toirano. *Bolletino*
967 *di Paletnologia italiana* Ser. II, t. VI, a. XVI, **1-2**: 1-16.
968 Negrino F, Tozzi C. 2008. Il paleolitico in Liguria. *Bull. Musée Anthropol. Préhistorique Monaco*
969 Suppl. **1**: 21-28.
970 Palmer, AN. 1987. Cave levels and their interpretation. *National Speleological Society Bulletin*, **49**:
971 50-66.
972 Palmer AN. 2007. Cave geology. Cave Books: Dayton (OH).
973 Piccini, L, De Waele, J, Galli, E, Polyak, VJ, Bernasconi, SM, Asmerom, Y. 2015. Sulphuric acid
974 speleogenesis and landscape evolution: Montecchio cave, Albegna river valley (Southern
975 Tuscany, Italy). *Geomorphology* **229**: 134-143.
976 Pirouelle F. 2006. *Contribution méthodologique à la datation, par les méthodes uranium-thorium*
977 *(U-Th) et résonance de spin électronique (ESR), de sites moustériens de Ligurie, de France et de*
978 *Belgique.* PhD Thesis, Muséum National d'Histoire Naturelle, Paris, 442 p.
979 Pozzi JP, Rousseau L, Falguères C, Mahieux G, Deschamps P, Shao Q, Kachi D, Bahain J-J, Tozzi
980 C. 2019. U-Th dated speleothem recorded geomagnetic excursions in the Lower
981 Brunhes. *Scientific Reports* **9**: Art. 1114: 1-8.
982 Rohling EJ, Foster GL, Grant KM, Marino G, Roberts AP, Tamisiea ME, Williams F. 2014. Sea-
983 level and deep-sea-temperature variability over the past 5.3 million years. *Nature* **508**(7497):
984 477-482.
985 Sarigu S. 2001. Il carsismo del complesso turistico di Toirano: descrizione strutturale, morfologica
986 e concrezionale. Ipotesi genetica per la grotta della Bàsura", *Atti V Convegno Speleologico*
987 *Ligure "Toirano 2000"*. Toirano, Italy; 149-156.

988 Sauro F, Mecchia M, Piccini L, De Waele J, Carbone C, Columbu A, Pisani L, Vergara F. 2019.
989 Genesis of giant sinkholes and caves in the quartz sandstone of Sarisariñama tepui, Venezuela.
990 *Geomorphology* **342**: 223-238.
991 Sauro F, Mecchia M, Tringham M, Arbenz T, Columbu A, Carbone C, Pisani L, De Waele J. 2020.
992 Speleogenesis of the world's longest cave in hybrid arenites (Krem Puri, Meghalaya, India).
993 *Geomorphology* **350**: 107-160.
994 Sasowsky ID. 1998. Determining the age of what is not there. *Science* **279**: 1874-1874.
995 Shen CC, Wu CC, Cheng H, Edwards RL, Hsieh YT, Gallet S, Chang CC, Li TY, Lam DD, Kano
996 A, Hori M, Spötl C. 2012. High-precision and high-resolution carbonate 230Th dating by MC-
997 ICP-MS with SEM protocols. *Geochimica et Cosmochimica Acta* **99**: 71-86.
998 Shen G. 1985. *Datation des planchers stalagmitiques de sites acheuléens en Europe par les*
999 *méthodes des déséquilibres des familles de l'uranium et contribution méthodologique.* PhD
1000 Thesis, Université Pierre et Marie Curie, Paris VI, 162 p.
1001 Soulet Q, Migeon S, Gorini C, Rubino J-L, Raisson F, Bourges P. 2016. Erosional versus
1002 aggradational canyons along a tectonically-active margin: The northeastern Ligurian margin
1003 (western Mediterranean Sea). *Marine Geology* **382**:17-36.
1004 http://dx.doi.org/10.1016/j.margeo.2016.09.015